

UNCLASSIFIED

AD NUMBER

ADB000524

LIMITATION CHANGES

TO:

Approved for public release; distribution is unlimited.

FROM:

Distribution authorized to U.S. Gov't. agencies only; Test and Evaluation; DEC 1974. Other requests shall be referred to Naval Ship Research and Development Center (Code 11), Bethesda, MD 2005.

AUTHORITY

USNSRDC ltr, 21 Sep 1977

THIS PAGE IS UNCLASSIFIED

THIS REPORT HAS BEEN DELIMITED
AND CLEARED FOR PUBLIC RELEASE
UNDER DOD DIRECTIVE 5200.20 AND
NO RESTRICTIONS ARE IMPOSED UPON
ITS USE AND DISCLOSURE.

DISTRIBUTION STATEMENT A

APPROVED FOR PUBLIC RELEASE;
DISTRIBUTION UNLIMITED.



NAVAL SHIP RESEARCH AND DEVELOPMENT CENTER

Bethesda, Md. 20084

ARCTIC SURFACE EFFECT VEHICLE PROGRAM

DATA ANALYSIS OF BAG/CUSHION HEAVE FORCES AND
PITCH MOMENTS ACTING ON A 10-TON SEV WHILE
CROSSING ISOLATED OBSTACLES

by

Samuel R. Shank, Jr. and James E. Hubbard

Sponsored by

DEFENSE ADVANCED RESEARCH PROJECTS AGENCY

ARPA Order No. 2251

Program Code No. 4N10

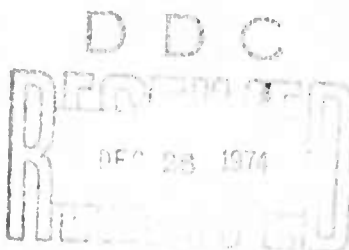
Distribution limited to U. S. Government agencies
only; Test and Evaluation; December 1974. Other
requests for this document must be referred to
Commander, Naval Ship Research and Development
Center (Code 11), Bethesda, Maryland 20034.

PROPULSION AND AUXILIARY SYSTEMS DEPARTMENT

Annapolis

EVALUATION REPORT

December 1974



Report PAS-74-27

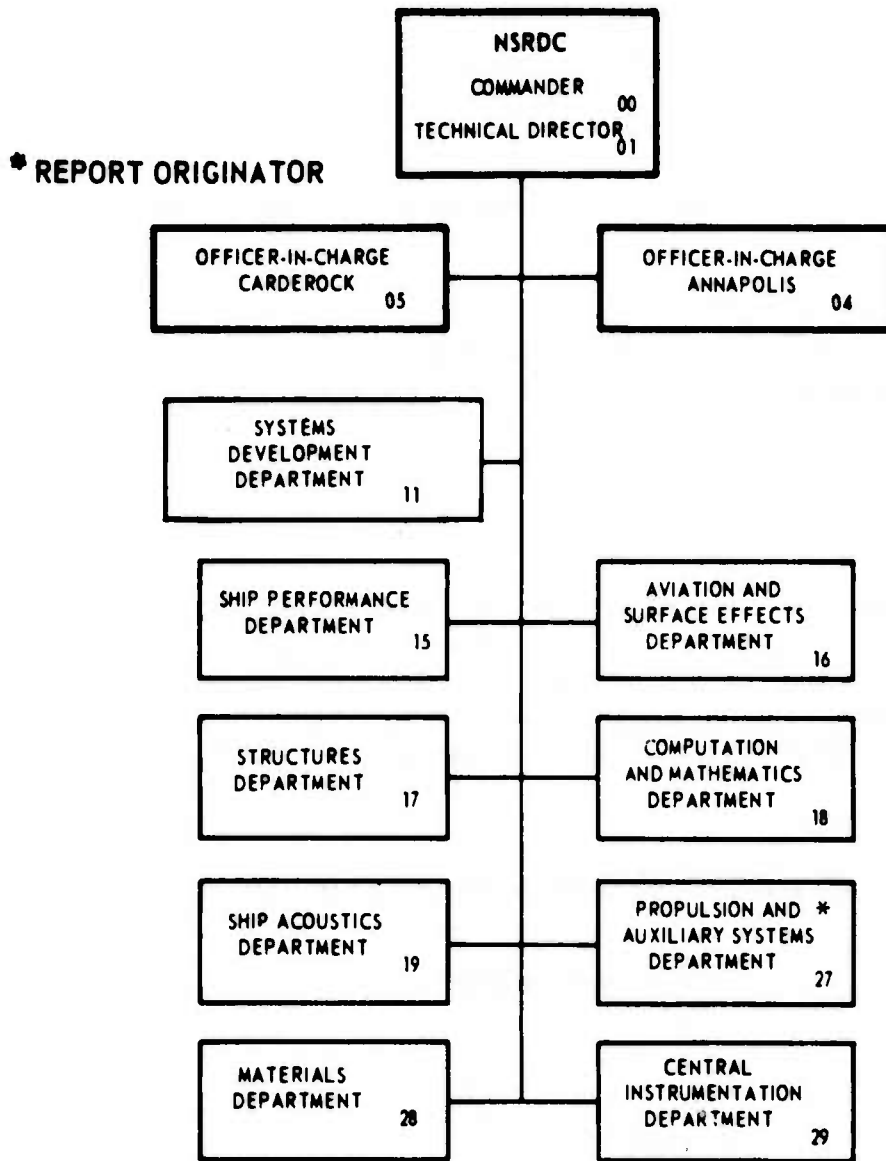
Data Analysis of Bag/Cushion Heave Forces and Pitch Moments Acting on a
10-Ton SEV While Crossing Isolated Obstacles

AD B 000524

The Naval Ship Research and Development Center is a U. S. Navy center for laboratory effort directed at achieving improved sea and air vehicles. It was formed in March 1967 by merging the David Taylor Model Basin at Carderock, Maryland with the Marine Engineering Laboratory at Annapolis, Maryland.

Naval Ship Research and Development Center
Bethesda, Md. 20034

MAJOR NSRDC ORGANIZATIONAL COMPONENTS



UNCLASSIFIED

SECURITY CLASSIFICATION OF THIS PAGE(When Data Entered)

ABSTRACT (Cont)

important in heave but not in pitch. Average bag heave forces on the order of 10% and 25% of vehicle weight are typical for the 0.5 and 1.0 obstacles, respectively. A detailed physical description of the cushion/obstacle interaction has resulted from the data analysis. Three major data trends - impact, venting, and slamming - are identified and related to cushion geometry. Bag effects have been correlated in terms of obstacle size, vehicle speed, and cushion geometry for ease of application as correction factors for analytical vehicle dynamics models based on cushion pressures only.

(Authors)

UNCLASSIFIED

SECURITY CLASSIFICATION OF THIS PAGE(When Data Entered)

ADMINISTRATIVE INFORMATION

This study was conducted for the Arctic Surface Effect Vehicle Program Office of the Naval Ship Research and Development Center through support provided by the Advanced Research Projects Agency of the Department of Defense. The work was performed in the Gas Turbines Branch of the Power Systems Division, Propulsion and Auxiliary Systems Department, under Work Unit 1-1130-300.

TABLE OF CONTENTS

	<u>Page</u>
ADMINISTRATIVE INFORMATION	i
NOTATIONS	v
INTRODUCTION	1
DATA	2
DATA ANALYSIS	5
Vehicle Heave/Pitch Motion	7
Cushion Heave Force/Pitch Moment	8
Bag Heave Force/Pitch Moment	8
Calculations	9
Reference Times	11
DISCUSSION OF RESULTS	12
Major Trends	14
CORRELATIONS	17
Trend Time Intervals	17
Heave Forces	21
Pitch Moments	23
CONCLUSIONS	26
RECOMMENDATIONS	27
TECHNICAL REFERENCES	27
APPENDIX	
Appendix A - Plots of Bag/Cushion Heave Forces and Pitch Moments (18 pages)	
INITIAL DISTRIBUTION	

NOTATION

- a_1 - vehicle vertical acceleration near center of gravity, ft/s²
- a_2 - vehicle vertical acceleration near bow, ft/s²
- a_y - vehicle heave acceleration, ft/s²
- α - vehicle pitch angular acceleration, rad/s²
- \bar{F} - average heave force within an interval, lb
- F_{BAG} - bag heave force, lb
- F_{CUSH} - cushion heave force, lb
- I - vehicle moment of inertia about pitch axis = 38,740 slug-ft²
- l_o - obstacle length, ft
- l_v - vehicle length, ft
- m - vehicle mass (= W/g), slugs
- \bar{M} - average pitch moment within an interval, lb-ft
- M_{BAG} - bag pitch moment, lb-ft
- M_{CUSH} - cushion pitch moment, lb-ft
- M_{THRUST} - thrust pitch moment, lb-ft
- P_1 - cushion gage pressures, forward starboard compartment, lb/ft²
- P_2 - cushion gage pressures, forward port compartment, lb/ft²
- P_3 - cushion gage pressures, rear port compartment, lb/ft²
- P_4 - cushion gage pressures, rear starboard compartment, lb/ft²
- r_1 - distance from center of gravity to a_1 accelerometer, ft
- r_2 - distance from center of gravity to a_2 accelerometer, ft
- Δt - impact, venting, or slamming time interval, s
- W - vehicle weight \approx 16,240 lb

Subscripts

- I - impact interval
- II - venting interval
- III - slamming interval
- T - sum of intervals, I, II, and III.

INTRODUCTION

The Advanced Research Projects Agency (ARPA) has established the high-speed surface effect vehicle (SEV) as an attractive concept for operation in the Arctic region. The vehicle must have long-range capability to enable it to traverse the thousands of unoccupied miles in the Arctic.

In order for this vehicle to be feasible, it must have a ride quality which is tolerable to its crew. Thus, it is necessary to develop motion prediction techniques to be used as vehicle design aids. A vehicle's dynamic motion is determined by a complex interaction of its cushion system with the terrain over which it is passing. The major items involved in this interaction are the cushion/fan elements and the bag which defines the cushion geometry. In most analyses, the assumption is made that the vehicle motion is small; no attention is paid to the forces transmitted to the vehicle due to bag contact with the terrain, and only cushion pressure changes are considered.

The purpose of this report is to provide a data base for bag effects, since this topic has not previously been evaluated. A method is developed for calculating the bag heave forces and pitch moments from vehicle acceleration and cushion pressure data. The bag forces and moments computed in this report represent the difference between measured cushion force and apparent total forces, as computed from vehicle accelerations. This method is applied to previously reported data¹ for discrete obstacles. The results of these calculations are used (1) to develop a detailed physical description of the cushion system/obstacle interaction and (2) to provide generalized bag effects data for use as correction factors to analytical models of vehicle dynamics based on cushion pressures only. Bag effects are considered significant when they are of the same order of magnitude as cushion effects.

No related references are available to be used as guidelines in the analysis and presentation of this material. It is hoped that the methodology chosen proves to be useful in terms of applying the bag results to augment previous analyses not accounting for bag effects.

¹ Superscripts refer to similarly numbered entries in the Technical References at the end of the text.

DATA

The bag and cushion effects analyses are made with previously reported data.¹ These data were obtained from a series of static and dynamic tests conducted on a refurbished and winterized SK-5 at the Naval Arctic Research Laboratory, Point Barrow, Alaska. The SK-5 is an 8-ton SEV, having an overall length of 38-1/2 feet and a beam of 24 feet. The SK-5 is powered by a General Electric LM 100 marine gas turbine engine. Propulsion is provided by a four-bladed, 9-foot-diameter, Dowty-Rotol propeller and lift by a 7-foot-diameter Westland Aircraft Limited centrifugal fan. Both propeller and fan are combined on the same shaft, with vehicle speed being controlled by using the propeller variable-pitch mechanism. The skirt system is a bag-finger type and air is continuously feed to it and to the air cushion by the fan. A more detailed description of the vehicle and of the objectives of the SK-5 test program is contained in the Program Overview.²

The experimental data¹ were obtained while the SK-5 was crossing different size obstacles at various speeds. The obstacles considered for this analysis were the 2-foot-high barrels and the 4-foot-high pile of beach gravel. Sketches of these obstacles are contained in figure 1. In both cases, the obstacle's lateral dimension exceeds the beam dimension of the SK-5. The length of the barrel obstacle (2 feet) is small in relation to the vehicle's length (38-1/2 feet) but the length of the gavel obstacle (16 feet) is not.

The overall cushion height of the SK-5 is approximately 5 feet plus a 6-inch air gap. The 5-foot cushion height includes a 1-foot-high finger. The obstacles thus provided a reasonable height variation when compared to the characteristic vehicle dimensions.

The data¹ include vehicle accelerations and cushion compartment pressures digitized from an analog tape in 0.01-second intervals. Figure 2 illustrates the location of the accelerometers and pressure transducers used to obtain the data. The gage pressures, P_1 , P_2 , P_3 , and P_4 , are measured in the four cushion compartments. The accelerations near the craft center of gravity (cg) and bow are designated a_1 , and a_2 , respectively.

Table 1 lists the pertinent identification of the data used in this report. This detailed information is given to facilitate synchronization of data in which this report with data appearing in other reports.

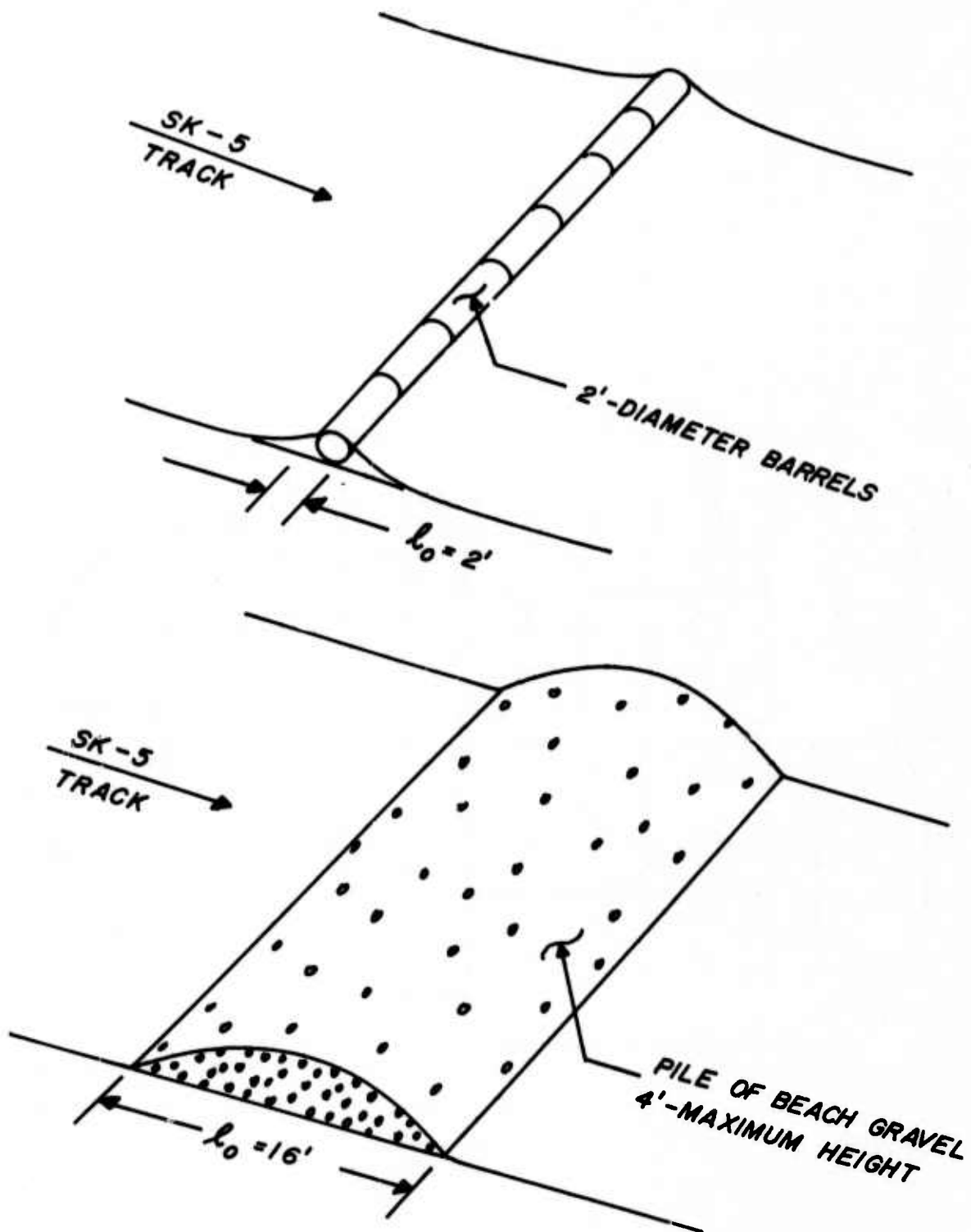


Figure 1
 Obstacles Considered in Bag and Cushion Force/Moment
 Comparisons

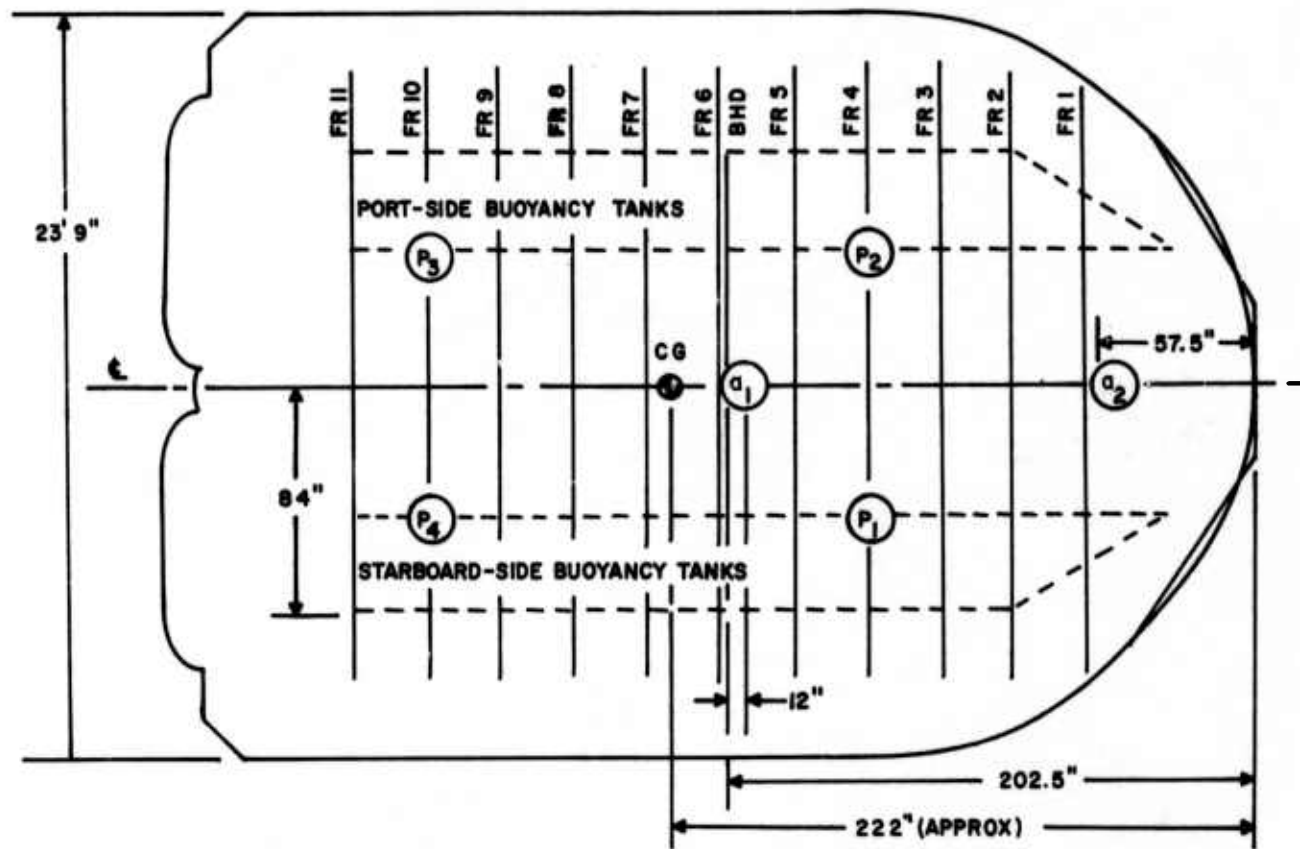


Figure 2
Accelerometer and Pressure Transducer Locations,
SK-5 Cushion Dynamics Data

TABLE 1
IDENTIFICATION OF DATA USED IN BAG/CUSHION
ANALYSIS

Analog Tape No.	Analog Run No.	Digital Tape No.	Digital File No.	Vehicle Velocity* knots	Obstacle Height ft	Reference Time**			
32835 ↓	1	CB1316 ↓	9	15	4 ↓	09/09/13.00			
	5		11	17		09/32/17.25			
	6		12	20		09/34/46.00			
	7		13	25		09/37/08.00			
	8		14	26		09/39/49.50			
	9		15	27		09/45/06.00			
	10		16	30		09/48/39.00			
	11		17	32		09/52/30.50			
	11A		18	32		11/03/02.50			
	12		19	16		11/10/43.50			
	32828 ↓		2	CB0222 ↓		8	14	2 ↓	09/40/15.50
			3			10	19		09/56/29.50
3A		11	17		11/11/50.50				
4		12	31		11/29/51.50				
5		14	34		11/40/20.00				
6		16	21		11/55/14.00				
7		17	13		11/06/33.00				
8		19	12		11/08/42.00				
<p>* These velocities have been calculated from the 24 and 450 frame per second 16-mm movies.</p> <p>** This time is given to provide an absolute time reference for all SK-5 data. It facilitates synchronization of this data with other data taken at the same time but appearing in other reports. The time given in this column corresponds with the 0.00 point or first piece of data in each graph of appendix A. The time is taken from the analog tape.</p>									

DATA ANALYSIS

The data are analyzed to yield heave forces and pitch moments. The vehicle motion, in response to the net forces and moments acting on it while traversing the obstacle, is calculated from the accelerations a_1 , and a_2 . Solid body translation and rotation is assumed. The heave forces and pitch moments acting on the vehicle, due to cushion pressure changes, are calculated from the gage pressures P_1 , P_2 , P_3 , and P_4 . In this calculation, the cushion compartment areas are assumed constant. (Evaluation of the

15-mm* film of the crossings and analysis of the bag geometry show that the maximum cushion-area change is 10% for short periods of time.) The remaining forces and moments acting on the vehicle are due to bag contact with the ground and are calculated from the equations of motion. Figure 3 shows a diagram useful for explaining the data reduction.

- | | |
|----------------------------|------------------------|
| A | - AREA |
| a | - ACCELERATION |
| P | - GAGE PRESSURE |
| r | - DISTANCE |
| α | - ANGULAR ACCELERATION |
| θ | - ANGLE |

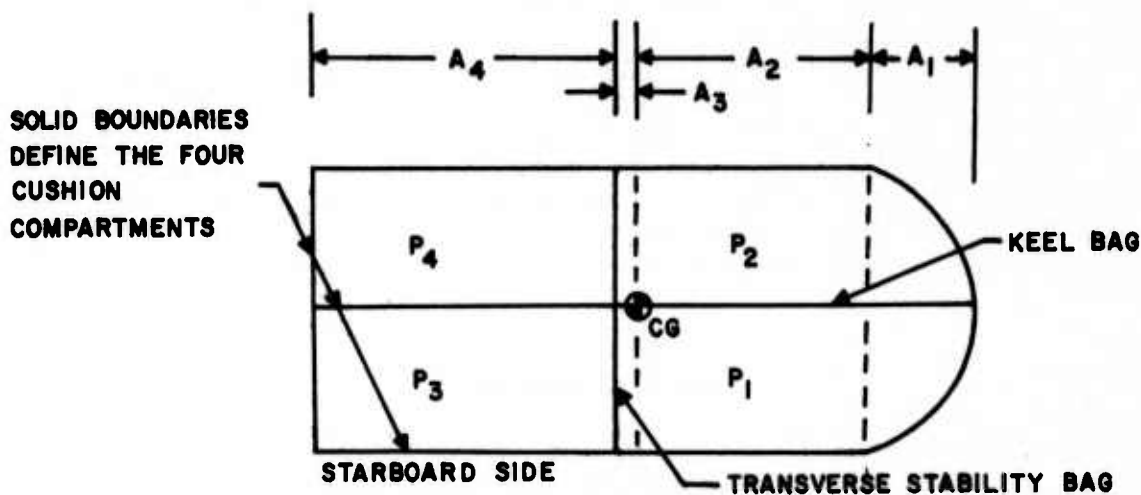
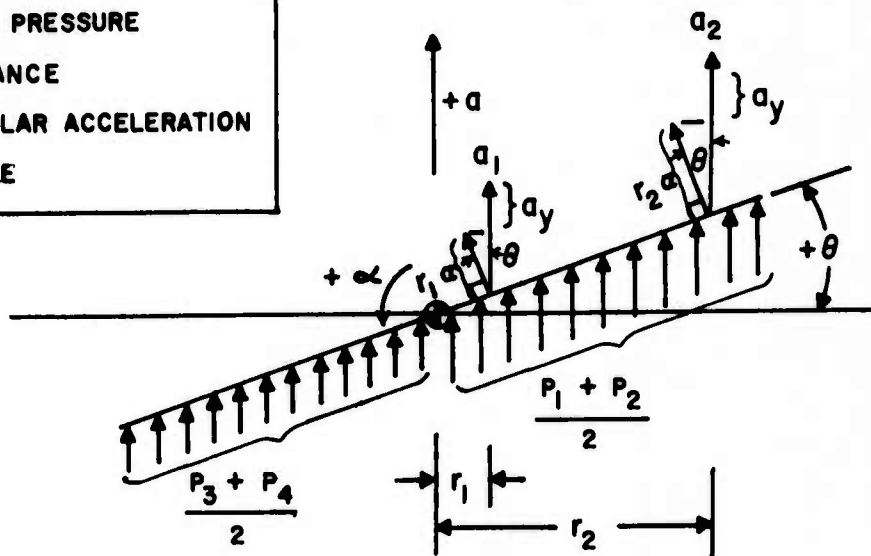


Figure 3
Data Reduction Rationale

* Abbreviations used in this text are from the GPO Style Manual, 1973, unless otherwise noted.

VEHICLE HEAVE/PITCH MOTION

Referring to figure 3, the accelerations (a_1, a_2) have two components, one related to heave and the other to pitch. The heave component for a_1 and a_2 , is the same (a_y) while the pitch components are proportional to the distance from the center of gravity; specifically:

$$a_1 = a_y + r_1 \alpha \cos \theta$$

and

$$a_2 = a_y + r_2 \alpha \cos \theta.$$

The above can be solved for α , the angular acceleration of the vehicle, to give

$$\alpha = \frac{a_2 - a_1}{(r_2 - r_1) \cos \theta}$$

If the angle θ is assumed to be small then,

$$\theta = \frac{a_2 - a_1}{r_2 - r_1},$$

and the heave acceleration a_y , is

$$a_y = a_1 - r_1 \frac{(a_2 - a_1)}{(r_2 - r_1)}.$$

Thus the heave acceleration (a_y) and pitch angular acceleration (α) are calculated from the data (a_1, a_2) and the distances (r_1, r_2) (obtainable from figure 2).

CUSHION HEAVE FORCE/PITCH MOMENT

The cushion heave force (F_{CUSH}) is obtained by summing the products of cushion compartment pressures and areas. Referring to figure 3,

$$F_{\text{CUSH}} = \left(\frac{P_1 + P_2}{2} \right) (A_1 + A_2 + A_3) + \left(\frac{P_3 + P_4}{2} \right) (A_4).$$

The cushion pitch moment acting on the vehicle is given by

$$M_{\text{CUSH}} = \left(\frac{P_1 + P_2}{2} \right) (A_1 x_1 + A_2 x_2 - A_3 x_3) - \left(\frac{P_3 + P_4}{2} \right) (A_4 x_4),$$

where x_1 , x_2 , x_3 , and x_4 are the absolute horizontal distances between the center of gravity of the vehicle and the centroids of the respective areas.

BAG HEAVE FORCE/PITCH MOMENT

In the heave equation of motion, the heave forces are made up of cushion and bag forces; that is,

$$F_{\text{CUSH}} + F_{\text{BAG}} = m a_y.$$

The mass of the vehicle (m) is known³ and it has been shown how the cushion heave force and vehicle heave acceleration can be calculated from the data. Thus, the bag force can be calculated from the heave equation of motion. It is the remainder when cushion forces are subtracted from the total force on the vehicle, as indicated by the heave acceleration.

Before the vehicle comes in contact with the obstacle, the bag force is essentially zero since little bag contact with the ground occurs, thus the vehicle motion is controlled by the

cushion pressure. This fact is utilized to make a small correction to the data. This correction accounts for either an error in cushion pressure or in calculation of cushion area or both.

The pitch equation of motion for the vehicle is:

$$M_{\text{CUSH}} + M_{\text{BAG}} + M_{\text{THRUST}} = I \alpha.$$

The calculation of the cushion moment and angular acceleration has been discussed. Unfortunately, data supplied by the thrust strain-gage type sensor were found to be random;¹ thus, the thrust moment is not known. It is known that the thrust during the pass over the obstacle was relatively constant since the propeller pitch was fixed and engine speed remained constant.¹ A constant thrust moment will be balanced by an equal but opposite cushion moment at some small trim angle of the vehicle. The vehicle's pitch motion is unaffected. For calculation purposes, an average thrust moment for the propeller, in the range of 15 to 30 knots, is substituted into the equation. The moment of inertia (I) is known.³ The bag pitch moment is calculated from the pitch equation of motion. It is the remainder when cushion moments are subtracted from the total moment on the vehicle, as indicated by the pitch accelerations.

CALCULATIONS

The many calculations were performed with the aid of previously developed SK-5 data-reduction computer programs.¹ Modifications made to these programs include the previously described calculations and provisions for plotting the bag/cushion heave forces and pitch moments as a function of time. The results were all plotted on the Cal Comp plotter* and are contained in their entirety in appendix A. Typical force and moment plots are shown in figures 4 and 5 for discussion purposes. Note that the forces and moments have been presented in dimensionless form for convenience. The heave forces are normalized with respect to the weight of the vehicle ($\approx 15,400$ pounds). Normalizing the pitch moments was not as straightforward. A reference-tipping moment (the nose-down moment which would occur if the vehicle were to extend over a shelf and the front cushion compartments were completely vented) was found to be convenient.

* The Cal Comp plotter is a graphical pen plotting system compatible with Fortran-oriented computer programs. The NSRDC plotter is driven offline through magnetic tape units.

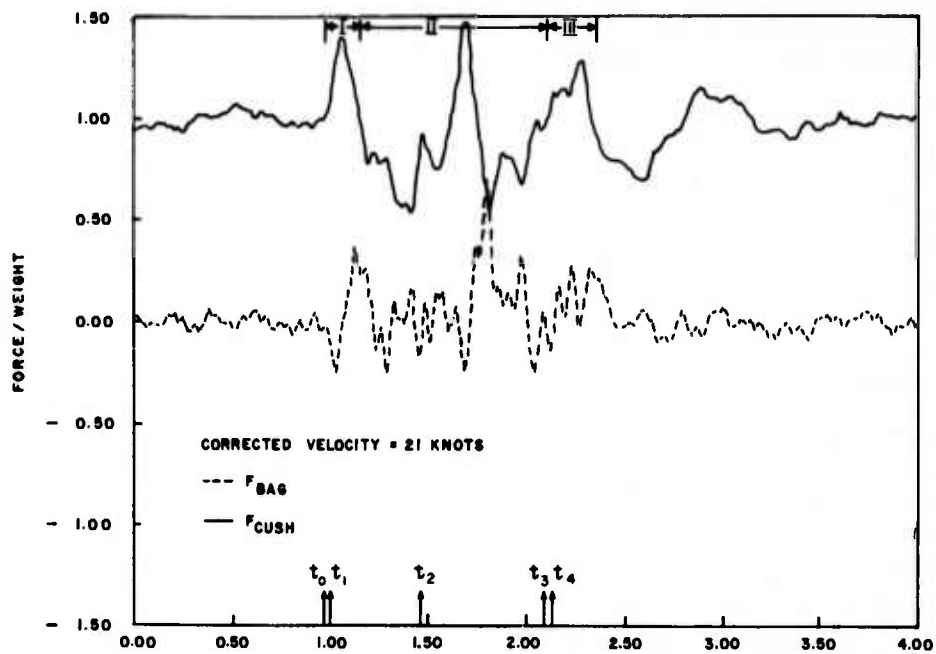


Figure 4
 Typical Bag/Cushion Heave Force Results
 (2-Foot Obstacle)

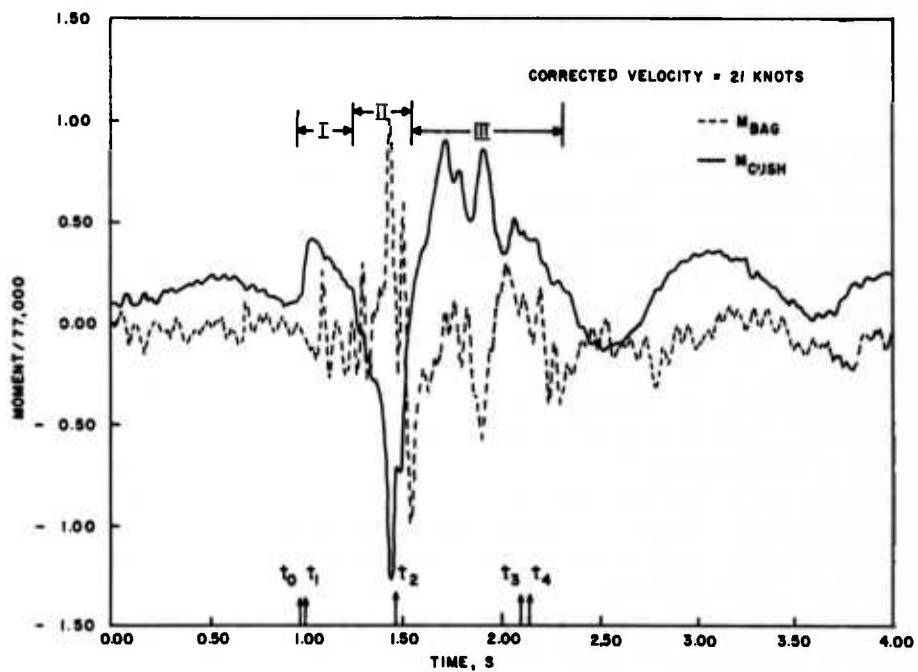


Figure 5
 Typical Bag/Cushion Pitch Moment Results
 (2-Foot Obstacle)

This reference-tipping moment is given by the product of half the vehicle weight (assumed to be uniformly distributed) times the distance from the pitch axis to the centroid of the area; specifically,

$$M_{\text{ref}} = \left(\frac{W}{2} \right) \left(\frac{l_v}{4} \right),$$

where

W = the vehicle weight
 l_v = the vehicle length ($l_v/4$ being the moment arm)
 $M_{\text{ref}} = 77,000$ ft-lb for the SK-5.

REFERENCE TIMES

Some reference times were established to facilitate data analysis. These times, defined below, are contained in figures 4 and 5.

t_0 = obstacle is encountered
 t_1 = vehicle bow reaches obstacle midpoint
 t_2 = vehicle transverse stability bag reaches obstacle midpoint
 t_3 = vehicle stern bag reaches obstacle midpoint
 t_4 = vehicle stern bag reaches the end of obstacle.

These times can all be calculated based on knowledge of the vehicle's velocity and the geometry of the vehicle and the obstacle. For example,

$$t_4 = t_0 + \frac{l_4}{V} = t_0 + \left(\frac{l_v + l_o}{V} \right)$$

where l_o = obstacle length.

For the case of the 2-foot obstacle, the times t_1 and t_3 are approximately the same as t_0 and t_4 , respectively, since the length of the 2-foot obstacle is small. Table 2 lists the reference times for all the data.

TABLE 2
OBSTACLE CROSSING REFERENCE TIMES

Digital Tape No.	Digital File No.	Vehicle Velocity knots	Obstacle Encountered	Bow Reaches Obstacle Midpoint	Transverse Stability Bag Reaches Obstacle Midpoint	Stern Bag Reaches Obstacle Midpoint	Stern Bag Reaches End of Obstacle
			t_0	t_1	t_2	t_3	t_4
↓	9	15	0.18	0.53	1.19	2.05	2.33
	11	17	0.74	1.05	1.63	2.39	2.64
	12	20	1.39	1.66	2.14	2.80	3.00
	13	25	1.38	1.59	1.98	2.50	2.67
	14	26	1.38	1.58	1.96	2.46	2.62
	15	27	1.70	1.90	2.26	2.74	2.90
	16	30	1.09	1.27	1.59	2.03	2.17
	17	32	1.59	1.76	2.06	2.47	2.60
	18	32	1.39	1.56	1.86	2.27	2.40
	19	16	0.99	1.32	1.93	2.75	3.00
	↓	8	14	1.59	1.63	2.32	3.26
10		19	1.59	1.62	2.14	2.82	2.85
11		17	1.52	1.55	2.13	2.90	2.93
12		31	1.39	1.41	1.72	2.14	2.16
14		34	1.02	1.04	1.32	1.71	1.73
16		21	0.98	1.01	1.47	2.09	2.12
17		13	0.98	1.02	1.78	2.78	2.82
19		12	1.10	1.15	1.96	3.05	3.10

Note that during the period of time before t_0 , the value of the cushion heave force is approximately unity and the bag heave force is approximately zero. This is typical of all the data and is obtained by making the small correction to the data previously discussed. These corrections averaged about 5% of the vehicle weight. Corrections to the moment data (figure 5) have not been made; therefore, the bag and cushion moments are not zero in the time interval before the obstacle is encountered. The reason for this is the unknown thrust moment and small errors in cushion pressure and cushion area which cannot be as easily corrected in the pitch sense as they were in the heave sense. The appropriate moment corrections are best made during correlation of the data.

DISCUSSION OF RESULTS

The results of all the heave force and pitch moment calculations are contained in appendix A. A discussion and analysis of this data is necessary in order to draw meaningful conclusions from it. A brief examination of these results reveals many similarities in the data. A preview of some

representative data for both obstacles is necessary to acquaint the reader with the data and to verify that it bears a physical relationship to the cushion/obstacle interaction. Figures 6 and 7 are representative of the 4-foot obstacle data as figures 4 and 5 are of the 2-foot obstacle data.

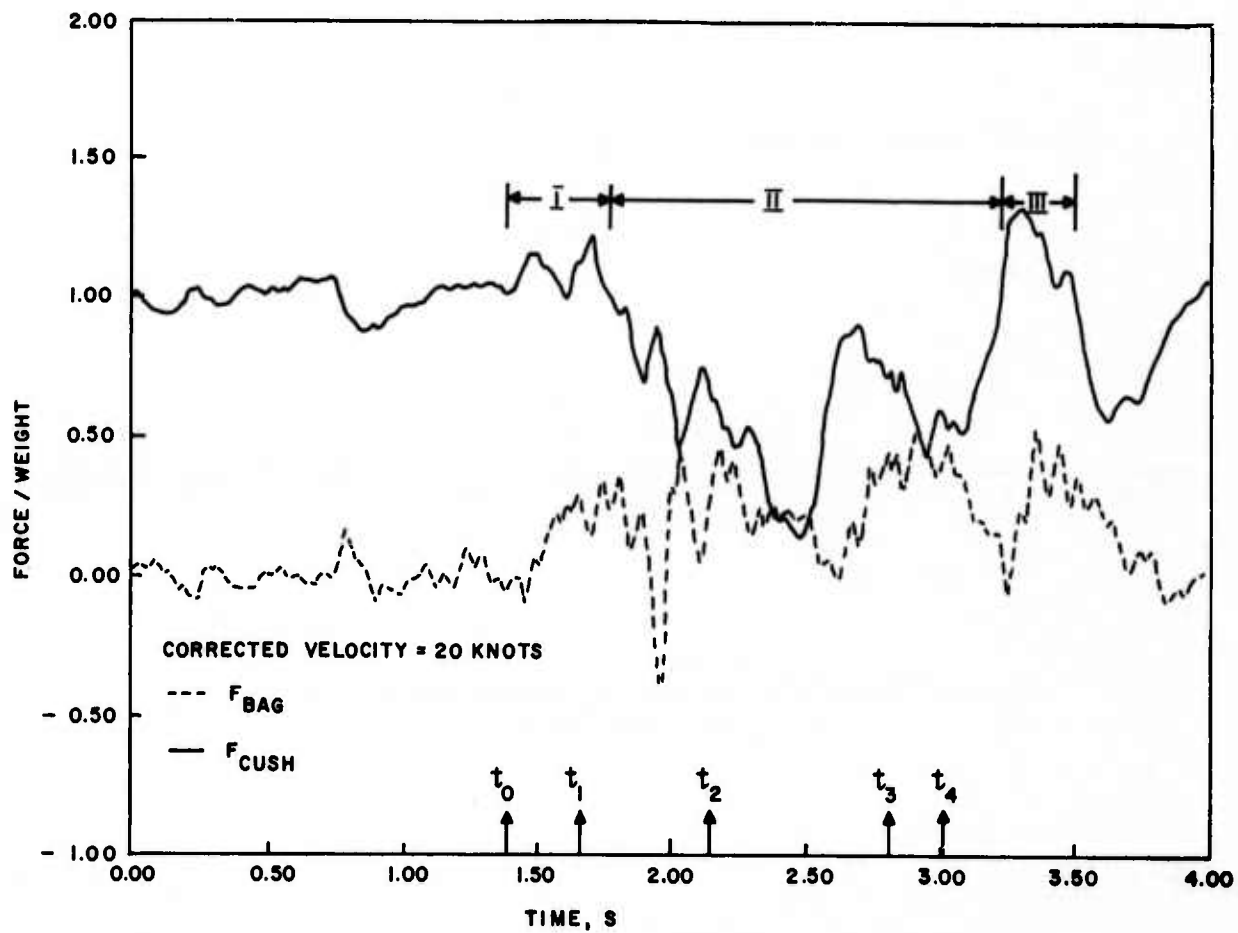


Figure 6
Typical Bag/Cushion Heave Force Results
(4-Foot Obstacle)

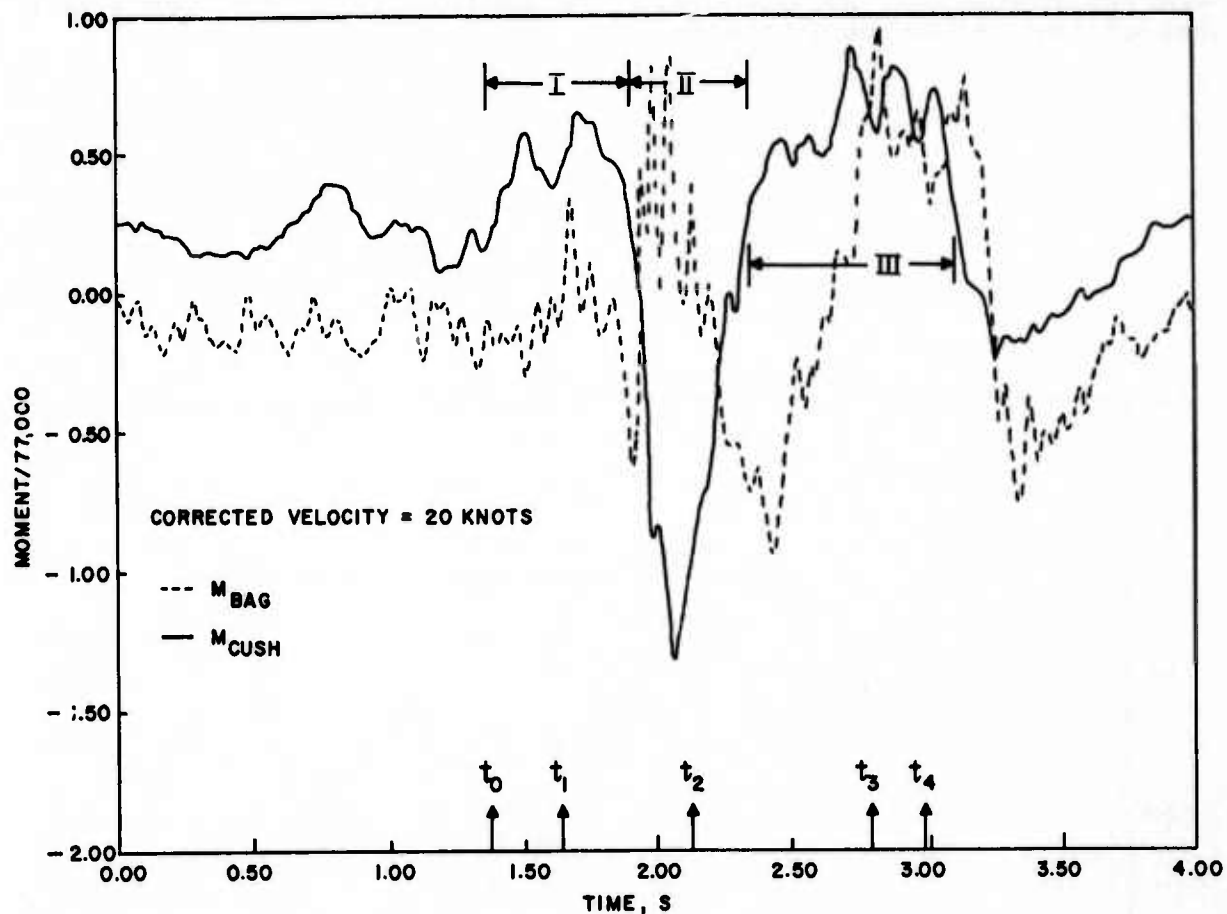


Figure 7
Typical Bag/Cushion Pitch Moment Results
(4-Foot Obstacle)

MAJOR TRENDS

Three major trends - impact, venting, and slamming - have been noted in both the heave forces and pitch moments. These major trends are most closely associated with the cushion forces and moments. The time periods associated with these three trends are not necessarily the same in heave as they are in pitch. The three intervals over which these trends occur are designated I, II, and III. These intervals are included in figures 4 through 7.

The first major trend (impact) in both heave and pitch occurs from t_0 to sometime between t_1 and t_2 . The time period in pitch is somewhat longer than the one in heave. The vehicle makes contact with the obstacle at t_0 , and pressures begin to rise in the front and rear cushion compartments because air is being forced into them from the compressed bag. The bag/finger skirt of the SK-5 is one continuous manifold (except at the stern) and has openings into all cushion compartments. The front compartments, being closer to the point of impact, receive more air than the rear compartments and therefore experience a faster pressure rise. Also, the volumes of the front cushion compartments are being somewhat decreased at impact, which further steepens their pressure rise. The positive pressure trend (positive-heave force) extends until sometime after t_1 when the front cushion compartments begin to vent. The end point of the first heave-force interval (I) is the time that cushion forces and moments cross the equilibrium values. A review of the 16-mm movies of the obstacle crossings shows that the bow bag tends to drag on the obstacle during impact, then release suddenly sometime after t_1 but before t_2 . Bag heave forces are generally calculated to be positive during this first interval, as would be expected, due to the compression of the bag in the bow area. Some discrete negative bag forces are calculated during this interval as well as in others. A small downward force could occur immediately upon impact due to the predominance of shear force on the bow bag before a large amount of bag compression occurs. Such a force appears in figure 4 at about t_1 for the 2-foot obstacle. This occurrence is not evident in any of the 4-foot obstacle data or in the low velocity 2-foot obstacle data. Further discussions of negative bag forces appear elsewhere.

Cushion moments are positive in the first moment interval, due to the accelerated pressure rise occurring in the front compartments. The sense of the bag moment is determined by the direction of the bag force resultant at the bow during impact.

The second major trend (venting) occurs in a time interval beginning sometime between t_1 and t_2 . The second heave interval (II) is much larger in duration than the pitch interval. At sometime after t_1 , the front cushion compartments begin to vent as the bow bag releases from the top of the obstacle. At this time, the cushion heave force drops suddenly below the equilibrium value. In the case of the 4-foot obstacle (figure 6), later venting of the rear compartments, coupled with only partial sealing of the front cushion compartments, combine to hold the cushion heave force below the equilibrium value until sometime after t_4 when all compartments seal. The sealing of the front compartment occurs between t_2 and t_3 , as shown by the rise in the cushion heave force in both the 2- and 4-foot cases. In the case of the 2-foot obstacle, the sealing of the front compartments is evidently complete since within the second interval the heave force exceeds the equilibrium value. The second interval for

pitch is short compared to the heave interval and ends sometime between t_2 and t_3 . The second pitch interval represents the negative cushion moment due to venting of the front cushion compartments. Bag moments in the pitch interval should be positive since the obstacle is forward of the center of gravity during most of this interval, and heave force data show that a large portion of vehicle weight is being supported by the bag.

It is of interest that some rather large oscillations in bag moment occur within this interval. These oscillations occur at around t_2 where only small bag moment effects are expected since the obstacle is centered under the vehicle. (It should be recalled that bag moments and forces are being calculated from accelerometer data.) Examination of these oscillations reveals that their period is independent of craft speed and corresponds to a 13.7-Hz structural resonance measured at the bow of the SK-5 in a mechanical shake test.⁴ This structural resonance appears to some degree in all of the bag moment data and to a lesser extent in the bag heave force data. Negative bag forces occurring in the data can be due to this structural resonance effect. It is most apparent at t_2 when approximately half of the vehicle is effectively cantilevered due to the complete venting of the front cushion compartments. The moment data calculated within the venting interval (II) is affected by this resonance. In the other two intervals, the resonance effects are small.

The third major trend (slamming) is associated with the resealing of the cushion after venting has occurred. In heave, this trend occurs in a time interval (III) beginning sometime after t_4 when all four cushion compartments seal. During the slamming interval, the pressure is rising in all four cushion compartments due to the sealing of the cushion and the cushion force is positive. The bag force is also positive as the cushion is compressed during sealing. In examining figures 4 and 6, it can be seen that the bag force characteristic is very similar in shape to the cushion force characteristic. It can be noted that some structural resonance effects are present at this time. In pitch, the slamming interval (III) begins after t_2 when partial sealing of the front cushion compartments has begun and the transverse stability bag has passed the obstacle midpoint initiating venting in the rear cushion compartments. These complementary effects impose a large positive cushion moment on the craft as shown in figures 5 and 7. In this interval, the bag moment is first negative as the rear section of the craft is on the obstacle and compression of the bag by the obstacle causes a moment in the negative sense. As the front cushion sealing progresses and bow bag compression occurs, the bag moment becomes positive within the slamming interval.

CORRELATIONS

The typical data preview has shown that the cushion/bag heave forces and pitch moments are related to the cushion/obstacle interaction. It now remains to correlate the data in a manner which allows for generalization of the results.

TREND TIME INTERVALS

The first items to be examined are the impact, venting, and slamming time intervals. As previously stated, the end points of these intervals are arbitrarily determined by the crossing of the cushion force/moment curves with the equilibrium heave force and pitch moment. The time intervals represent a convenient way of grouping the data but are subject to errors of judgment. Correlations of these time intervals with vehicle velocity are shown in figure 8. The times shown in figure 8 are the time intervals (Δt_I , Δt_{II} , Δt_{III}) and the total time (Δt_T) for the three time intervals. These data appear in tables 3 and 4. The time-interval data is correlated in figure 8 by dividing them by a reference time interval ($t_4 - t_0$) associated with the vehicle length and obstacle length; that is,

$$t_4 - t_0 = \frac{l_v + l_o}{v} .$$

The correlations of figure 8 are good and show the similarity of the data from run to run, thus justifying the choice of time intervals. The correlations show that the heave and pitch impact intervals (I) are about the same and vary from 10% to 40% of the reference time interval. The heave venting interval (II) is approximately 80% of the reference interval, while the pitch venting interval (II) is about half that duration. This is due to the fact that repressurization of the front cushion compartments, coupled with venting of the rear cushion compartments, causes positive moments and negative heave forces; thus, the period of time while this is occurring is called venting in heave, but slamming in pitch. It follows then that the slamming interval (III) in heave will be smaller than in pitch, and this is verified in figure 8. The heave slamming interval approaches 50% of the reference interval while the pitch interval approaches 90%. The total time intervals for both heave and pitch (Δt_T) are about the same. At the lower velocities, Δt_T is about equal to the reference interval while at the higher speeds Δt_T approaches 1.5 times the reference interval.

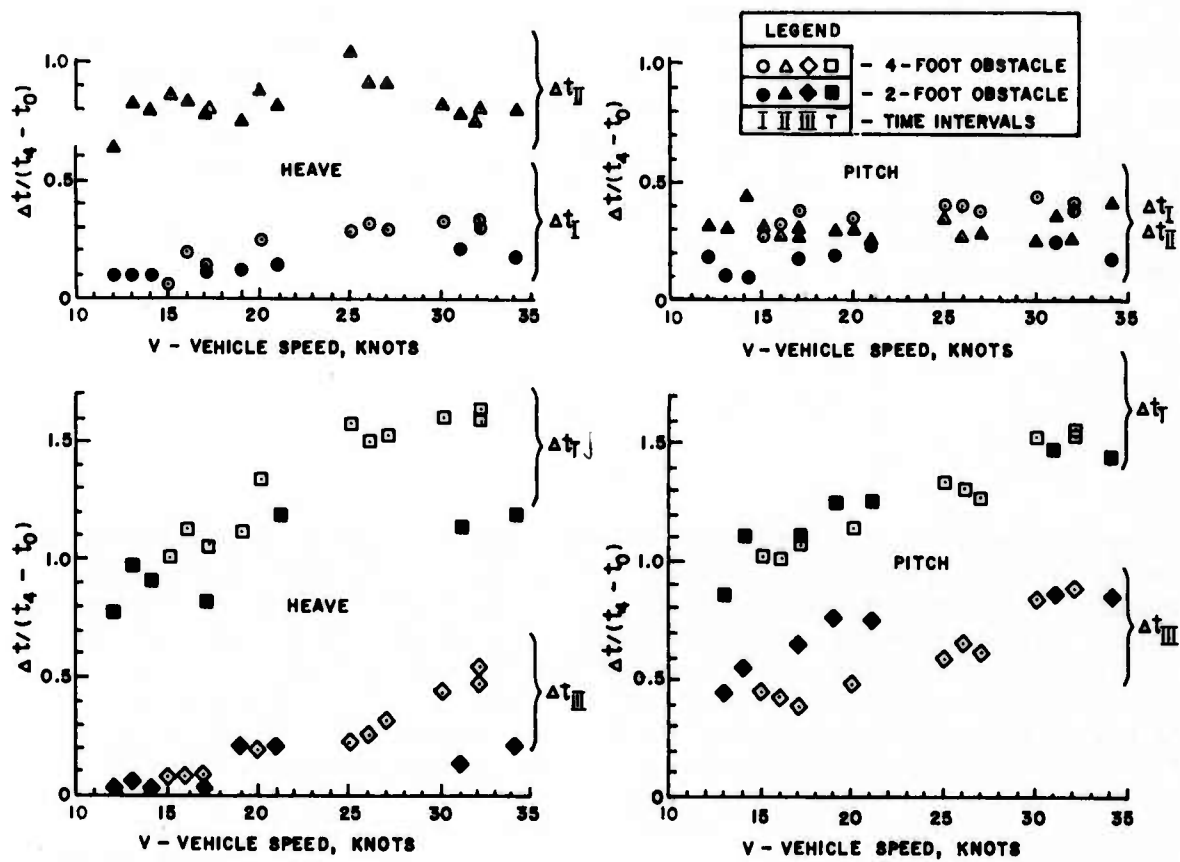


Figure 8
Correlations of the Impact, Venting and
Slamming Time Intervals

TABLE 3
CUSHION HEAVE-FORCE DATA SUMMARY

Digital Tape No.	Digital File No.	Vehicle Velocity knots	I		II		III	
			Δt_I	\bar{F}/W	Δt_{II}	\bar{F}/W	Δt_{III}	\bar{F}/W
CB1316 ↓	9	15	0.14	0.075	1.85	-0.410	0.18	0.148
	11	17	0.28	0.070	1.52	-0.351	0.20	0.200
	12	20	0.41	0.110	1.42	-0.381	0.33	0.179
	13	25	0.37	0.157	1.36	-0.411	0.30	0.221
	14	26	0.40	0.228	1.14	-0.418	0.32	0.239
	15	27	0.35	0.221	1.11	-0.415	0.38	0.200
	16	30	0.36	0.342	0.90	-0.497	0.47	0.231
	17	32	0.33	0.411	0.76	-0.594	0.56	0.290
	18	32	0.30	0.375	0.82	-0.547	0.31	0.275
	19	16	0.41	0.096	1.68	-0.346	0.19	0.289
CB0222 ↓	8	14	0.17	0.119	1.36	-0.091	0.04	0.041
	10	19	0.16	0.166	0.97	-0.115	0.28	0.061
	11	17	0.15	0.198	0.97	-0.084	0.05	0.071
	12	31	0.16	0.310	0.61	-0.238	0.11	0.333
	14	34	0.13	0.414	0.56	-0.321	0.15	0.337
	16	21	0.17	0.240	0.95	-0.128	0.24	0.161
	17	13	0.19	0.113	1.50	-0.091	0.11	0.045
	19	12	0.19	0.075	1.30	-0.076	0.05	0.034

TABLE 4
CUSHION PITCH MOMENT DATA SUMMARY

Digital Tape No.	Digital File No.	Vehicle Velocity knots	I		II		III	
			Δt_I	\bar{M}/M_{ref}	Δt_{II}	\bar{M}/M_{ref}	Δt_{III}	\bar{M}/M_{ref}
CB1316 ↓	9	15	0.58	0.091	0.65	-0.651	0.96	0.215
	11	17	0.72	0.083	0.55	-0.675	0.75	0.225
	12	20	0.56	0.209	0.50	-0.890	0.77	0.345
	13	25	0.52	0.201	0.45	-0.836	0.76	0.308
	14	26	0.49	0.288	0.32	-1.074	0.81	0.428
	15	27	0.45	0.257	0.34	-1.003	0.73	0.469
	16	30	0.48	0.331	0.27	-0.932	0.91	0.410
	17	32	0.41	0.399	0.26	-0.911	0.89	0.334
	18	32	0.38	0.350	0.26	-0.857	0.90	0.275
	19	16	0.65	0.179	0.55	-0.703	0.84	0.212
CB0222 ↓	8	14	0.17	0.062	0.77	-0.096	0.94	0.196
	10	19	0.24	0.069	0.39	-0.186	0.94	0.242
	11	17	0.25	0.113	0.38	-0.163	0.91	0.265
	12	31	0.19	0.194	0.28	-0.553	0.66	0.281
	14	34	0.13	0.263	0.29	-0.516	0.60	0.349
	16	21	0.27	0.163	0.30	-0.505	0.86	0.244
	17	13	0.21	0.073	0.55	-0.206	0.81	0.191
	19	12	0.35	0.046	0.64	-0.116	-	-

HEAVE FORCES

The next items to be examined are the average heave forces of tables 3 and 5. The heave forces tabulated are differentials from the equilibrium value. Correlations of these forces with vehicle speed are shown in figure 9 with the three intervals of interest.

TABLE 5
BAG HEAVE FORCE DATA SUMMARY

Digital Tape No.	Digital File No.	Vehicle Velocity knots	I		II		III	
			Δt_I	\bar{F}/W	Δt_{II}	\bar{F}/W	Δt_{III}	\bar{F}/W
CB1316 ↓	9	15	0.14	-0.027	1.85	0.262	0.18	0.157
	11	17	0.28	0.002	1.52	0.227	0.20	0.155
	12	20	0.41	0.072	1.42	0.246	0.33	0.226
	13	25	0.37	0.142	1.36	0.262	0.30	0.239
	14	26	0.40	0.170	1.14	0.204	0.32	0.304
	15	27	0.35	0.217	1.11	0.178	0.38	0.328
	16	30	0.36	0.180	0.90	0.128	0.47	0.278
	17	32	0.33	0.169	0.76	0.085	0.56	0.182
	18	32	0.30	0.150	0.82	0.108	0.31	0.286
	19	16	0.41	0.089	1.68	0.237	0.19	0.227
CB0222 ↓	8	14	0.17	0.059	1.36	0.075	0.04	-0.072
	10	19	0.16	0.062	0.97	0.090	0.28	0.029
	11	17	0.15	0.022	0.97	0.054	0.05	-0.117
	12	31	0.16	0.031	0.61	0.086	0.11	0.070
	14	34	0.13	0.039	0.56	0.059	0.15	0.066
	16	21	0.17	0.052	0.95	0.096	0.24	0.110
	17	13	0.19	0.068	1.50	0.063	0.11	0.012
	19	12	0.19	0.050	1.30	0.054	0.05	0.115

In figure 9, the circles represent cushion heave-force data and the triangles represent bag heave force data. The empty symbols are used for the 4-foot obstacle and the filled symbols are used for the 2-foot obstacles. When the interval of interest was less than 0.1 second, the bag forces were not plotted.

In the impact interval (item (a), figure 9), the cushion forces increase with velocity. This is reasonable since both mechanisms contributing to this force (bag air forced into the cushion compartments and displacement of cushion volume by the obstacle) are velocity dependent. It is interesting that the magnitude of average cushion heave force is about the same for

both obstacles. Significant bag forces, on the order of 50% to 100% of cushion forces are calculated for the 4-foot obstacle but not for the 2-foot obstacle. This could be because the air gap and fingers are forgiving for this obstacle size and smaller. In the impact interval, the vehicle heave accelerations will then be a function of obstacle size and the obstacle size affects bag forces more than cushion forces.

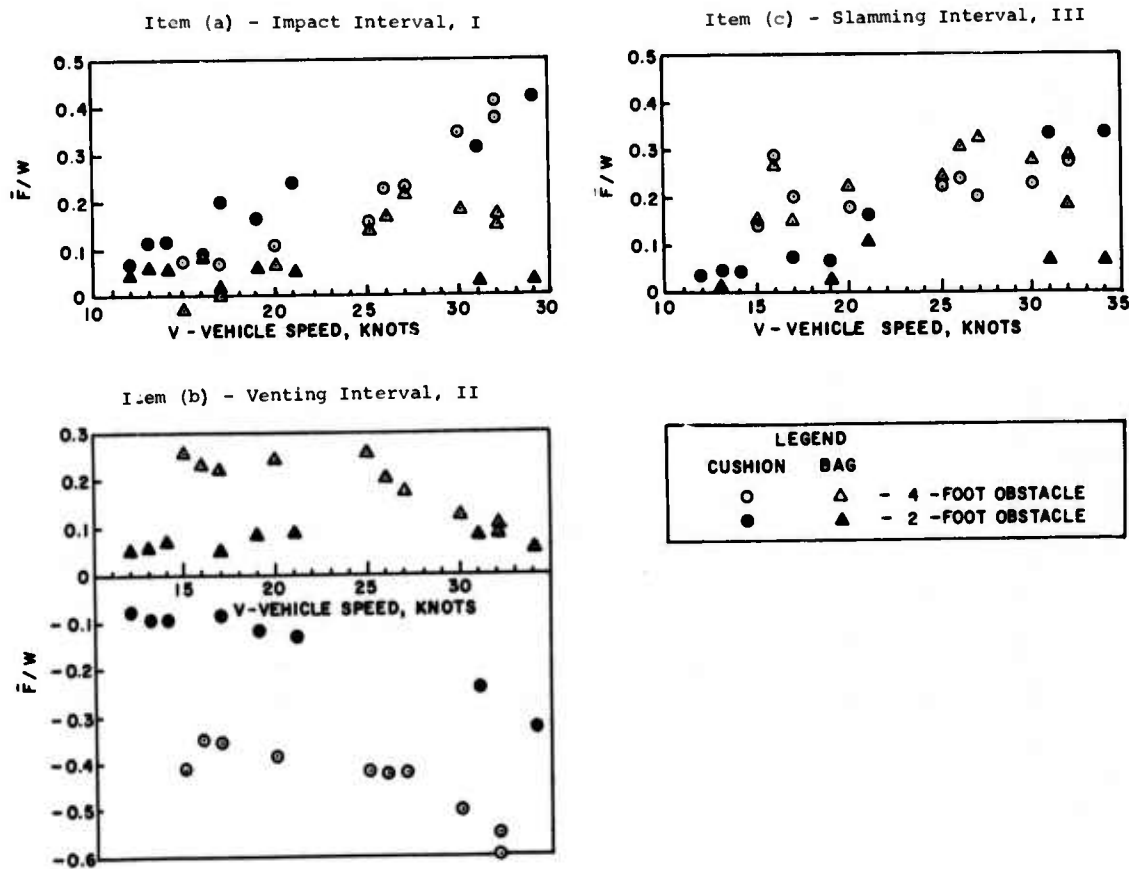


Figure 9
Correlations of the Impact, Venting, and
Slamming Heave Forces

In the venting interval (item (b), figure 9) both the bag and cushion forces are functions of obstacle size. The cushion force in this interval is negative since the pressure in the cushion compartments is decreasing due to the venting. At the lower speeds (less than 25 knots), the average cushion force is

independent of speed but varies significantly with obstacle size since venting area is related to obstacle size. At the higher speeds, the cushion forces have some velocity dependence. The 16-mm movies show that the vehicle actually does some "flying" at speeds of 25 knots and above; that is, the vehicle has enough momentum to remain in the air for a period of time after it has cleared the obstacle midpoint. The flying is more noticeable with the 4-foot obstacle than it is with the 2-foot one. The negative cushion force over the entire venting interval causes the vehicle to move downward and bag compression and therefore bag forces occur. The bag forces are significant (of the same magnitude as the cushion forces) as shown in item (b) of figure 9. It is interesting that the bag force for the 4-foot obstacle case actually decreases at the higher velocities. This is again due to the flying of the vehicle, preventing the bag skirts from ground contact over a large portion of the venting time interval, and thus reducing the average bag heave force over the entire interval.

Cushion forces and bag forces in the slamming interval (item (c), figure 9) are very similar to those of the impact interval. The cushion forces increase with vehicle velocity and appear to be independent of obstacle size. For the 2-foot obstacle, bag heave forces are insignificant; however, for the 4-foot obstacle they are of the same order of magnitude as the cushion forces as shown in item (c) of figure 9. This large bag force is associated with the flying of the vehicle and due to the large bag compression which occurs as the vehicle "lands," the cushion compartments seal, and a concurrent rise in cushion pressure occurs.

In summary, bag heave forces are significant in the venting zone for the 2-foot obstacle case where the obstacle-to-cushion height ratio is about 1/2. For the 4-foot obstacle, where the height ratio is about unity, the bag heave forces are significant in all three zones. Bag forces on the order of 25% of vehicle weight are typical. With bag pressures on the order of 50 lb/ft², this weight can be supported with a 7-inch uniform bag contact width. Structural resonance effects have been minimized by looking at the average bag heave forces.

PITCH MOMENTS

The next items to be examined are the average pitch moments of tables 4 and 6. The moments tabulated are differentials from the equilibrium value. Correlations of these moments with vehicle speed are shown in figure 10 for the three intervals of interest. In figure 10, the circles represent cushion pitch moment data and the triangles represent bag pitch moment data. The empty symbols are used for the 4-foot obstacle and the filled symbols are used for the 2-foot obstacle. Again, by looking at the average moments, the structural resonance effects are minimized.

TABLE 6
BAG PITCH MOMENT DATA SUMMARY

Digital Tape No.	Digital File No.	Vehicle Velocity knots	I		II		III	
			Δt_I	\bar{M}/M_{ref}	Δt_{II}	\bar{M}/M_{ref}	Δt_{III}	\bar{M}/M_{ref}
CB1316 ↓	9	15	0.58	0.045	0.65	-0.073	0.96	0.135
	11	17	0.72	0.039	0.55	0.069	0.75	0.297
	12	20	0.56	0.041	0.50	0.086	0.77	0.245
	13	25	0.52	0.015	0.45	0.093	0.76	0.238
	14	26	0.49	0.033	0.32	0.221	0.81	0.137
	15	27	0.45	0.063	0.34	0.182	0.73	0.123
	16	30	0.48	-0.067	0.27	0.095	0.91	-0.005
	17	32	0.41	-0.059	0.26	0.122	0.89	0.032
	18	32	0.38	-0.103	0.26	0.170	0.90	0.007
19	16	0.65	0.005	0.55	0.127	0.84	0.140	
CB0222 ↓	8	14	0.17	-0.023	0.77	0.016	0.94	-0.121
	10	19	0.24	-0.033	0.39	0.024	0.94	-0.124
	11	17	0.25	-0.064	0.38	-0.005	0.91	-0.138
	12	31	0.19	-0.042	0.28	0.042	0.66	-0.172
	14	34	0.13	-0.111	0.29	0.027	0.60	-0.203
	16	21	0.27	-0.053	0.30	0.059	0.86	-0.095
	17	13	0.21	0	0.55	-0.005	0.81	-0.068
	19	12	0.35	0.034	0.64	0.005	-	-

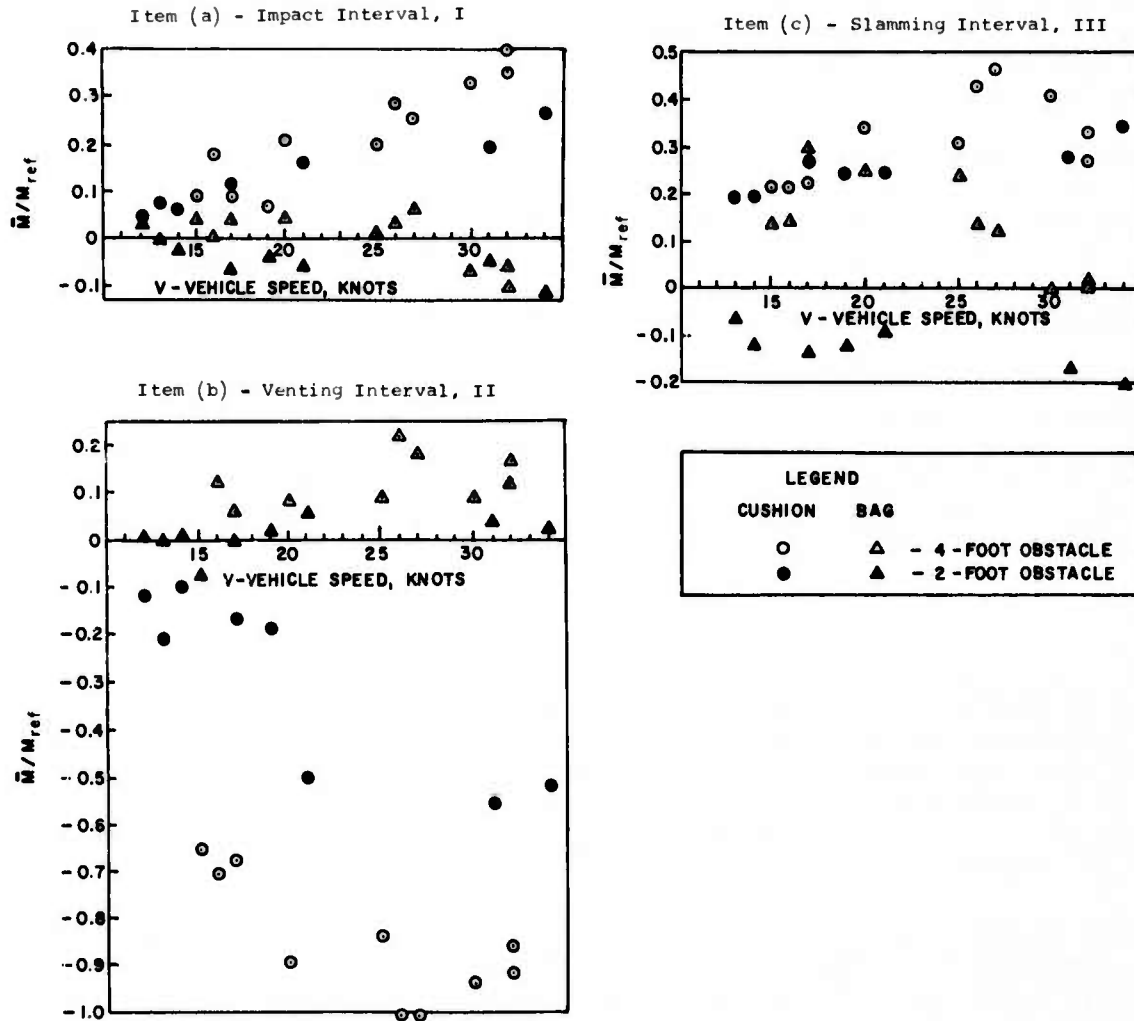


Figure 10
Correlation: of the Impact, Venting, and
Slamming Pitch Moments

In the impact interval (item (a), figure 10), the cushion moments for both obstacles increase with vehicle velocity. The cushion moments for the 4-foot obstacle somewhat exceed those of the 2-foot obstacle. Bag moments are not significant in this interval for either obstacle, although some small negative moments are calculated, possibly due to shear force on the bag when in contact with the ground or obstacle.

In the venting interval (item (b), figure 10), the cushion moments are again dominant. In this interval, the cushion moments are negative due to the venting of the front cushion compartments. The cushion moments increase in magnitude with velocity. It is

not expected that this moment could greatly exceed -1.0 (i.e., the reference moment) but higher velocity data would be necessary to verify this. The negative cushion moments are also a function of obstacle size, as shown in item (b), figure 10. Bag moments in the venting interval are not significant for either obstacle.

The slamming interval (item (c), figure 10) is similar to the impact interval except that some significant bag moments did exist at around 20-25 knots for the 4-foot obstacle. At higher speeds, the cushion moments dominated. Negative bag moments were again calculated for the 2-foot obstacle but in general were less than 50% of the magnitude of the cushion moments.

In summary, bag pitch moments are not significant for the 2-foot obstacle case, although in the impact and slamming intervals the bag moment tended to reduce the effect of the cushion moment. For the 4-foot obstacle, a few significant bag moments appeared in the slamming interval over the narrow speed range of 20-25 knots. The bag effects are more important in heave than they are in pitch.

CONCLUSIONS

A method for evaluating the magnitude of bag effects on the vehicle dynamics of an SEV has been developed. The method involves the calculation of bag heave forces and pitch moments from vehicle acceleration and cushion pressure data. The method has been applied to an SK-5 crossing discrete obstacles, having heights equal to 50% and 100% of the cushion height. The method is not limited to discrete obstacles.

A detailed physical description of the cushion/obstacle interaction has resulted from the data analysis. Three major trends - impact, venting, and slamming have been identified. The SK-5 cushion is considered representative of most SEV cushion configurations.

Structural resonance effects have been identified particularly at the time when the front cushion compartments are venting and half the vehicle is effectively cantilevered. The resonance effects prevent the accurate calculation of maximum bag forces and moments. By considering average forces and moments, over intervals larger than the period of the resonance, the effects are minimized.

Bag effects (as compared to cushion effects) are important in heave but not in pitch for the cases examined. The magnitudes of the bag heave forces are dependent on vehicle velocity and obstacle size. Average bag heave forces on the order of 10% and 25% of vehicle weight are typical for the 2- and 4-foot obstacles, respectively. With bag pressures on the order of 50 lb/ft², a 7-inch uniform bag contact width will support 25% of the weight of the SK-5.

The bag effects have been correlated in terms of obstacle size and vehicle speed. The correlations have been performed for the impact, venting, and slamming intervals which are related to cushion geometry. The data have been generalized in this manner for ease of application as a correction factor to analytical models of vehicle dynamics based on cushion pressures only.

RECOMMENDATIONS

The results of this analysis should be used to correct the vehicle dynamics predictions of analytical models based on cushion pressures only.

More such detailed analyses of cushion system/obstacle interaction should be performed using the reported method to improve the correction capability for any design.

TECHNICAL REFERENCES

- 1 - Shank, S. R., Jr., and J. S. Houston, "10-Ton SEV Obstacle-Crossing Data Related to Cushion System Dynamics," NSRDC Rept 27-229 (Aug 1972)
- 2 - "Arctic Surface Effect Vehicle Program, Overview of SK-5 Barrow Alaska Tests," prepared by Systems Development Dept., Arctic SEV Program Office, NSRDC (Aug 1971)
- 3 - Howe, H. J., and J. M. Durkin, "Preliminary Results of a 10-Ton Surface Effect Vehicle in the Arctic, Discrete Obstacle Cro-sing (Data Rept 161-4)," NSRDC Tech Note AL-244 (Jan 1972)
- 4 - Hagen, Adrian, "Mechanical Shake Test of an SK-5 Air Cushion Vehicle," NSRDC Rept SAD-3TE-1962 (Jan 1972)

APPENDIX A

PLOTS OF BAG/CUSHION HEAVE FORCES AND PITCH MOMENTS

PAS-74-27

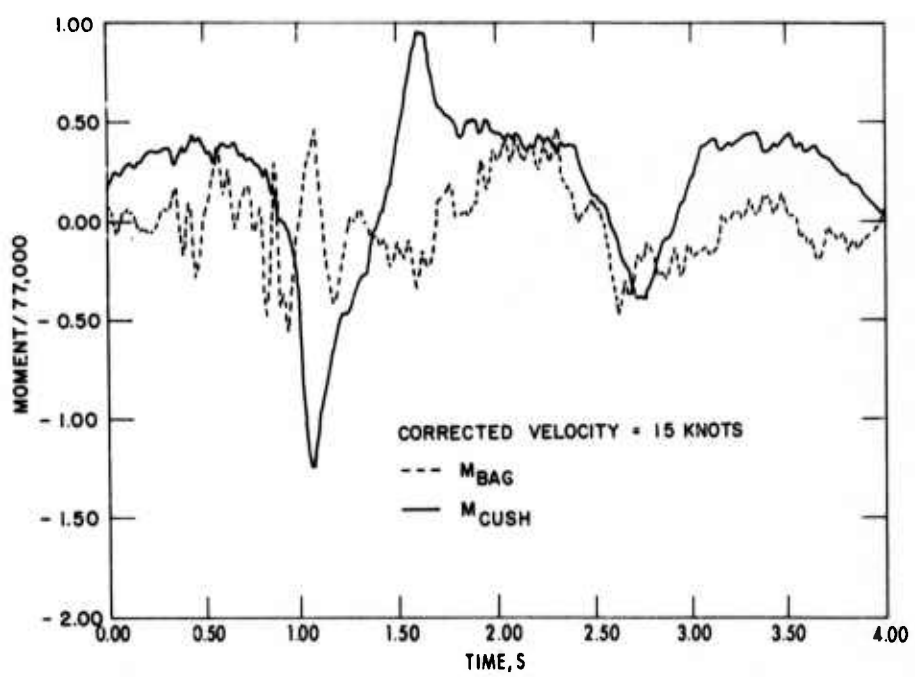
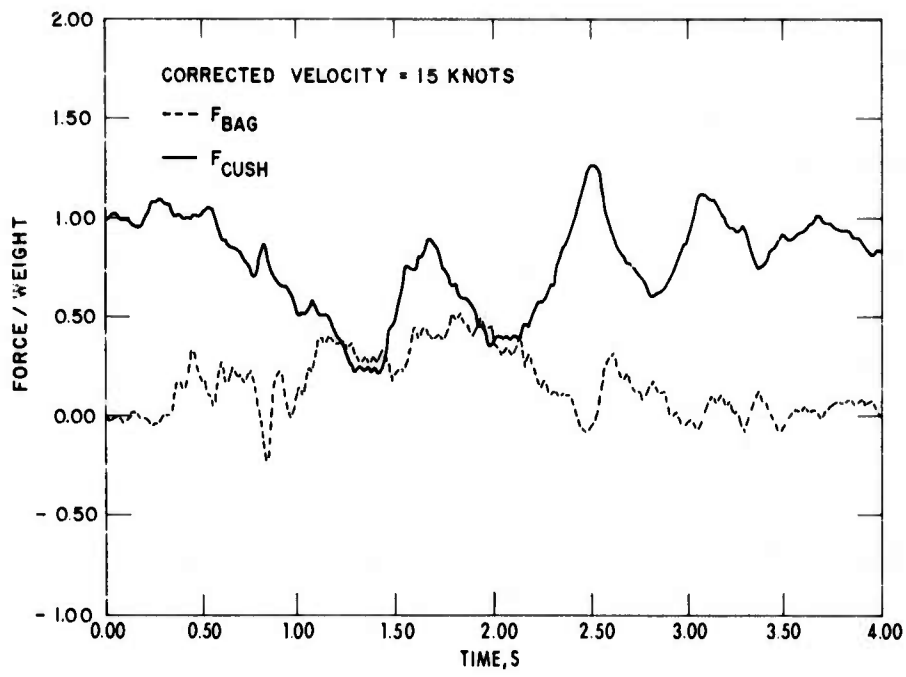


Figure 1-A
 Bag/Cushion Heave Forces and Pitch Moments
 4-Foot Obstacles (15 Knots)

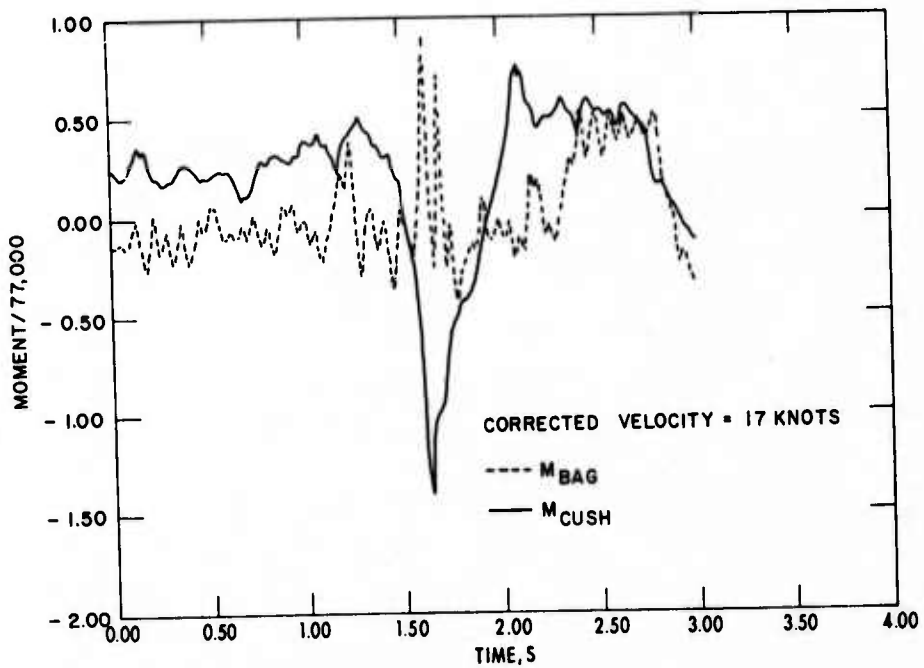
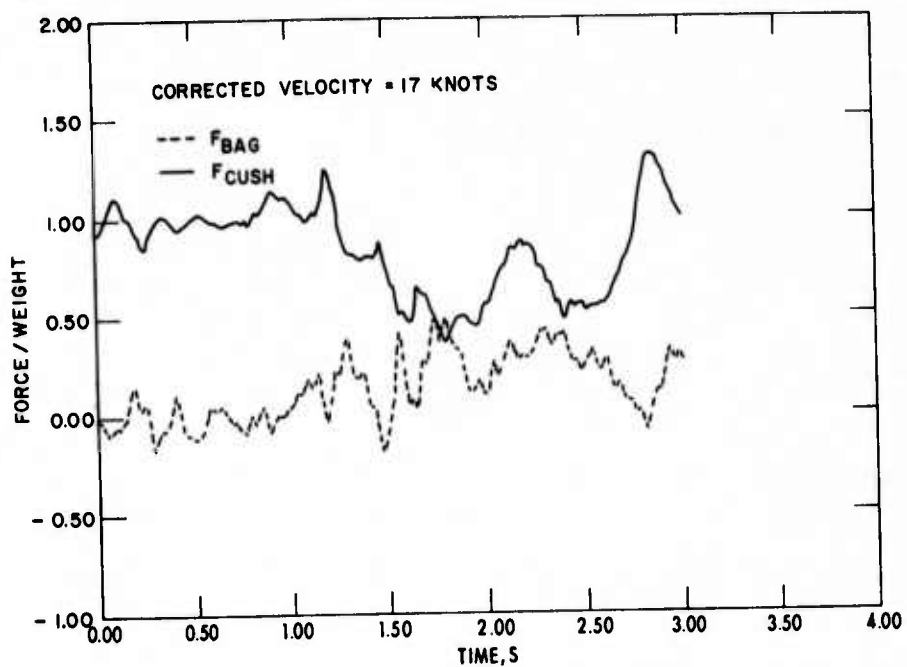


Figure 2-A
Bag/Cushion Heave Forces and Pitch Moments
4-Foot Obstacle (17 Knots)

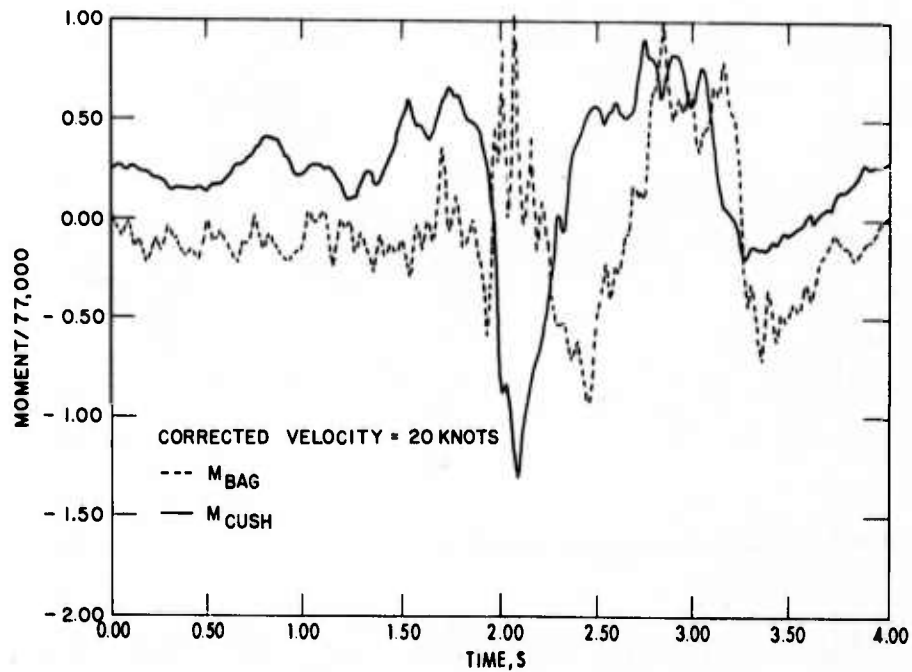
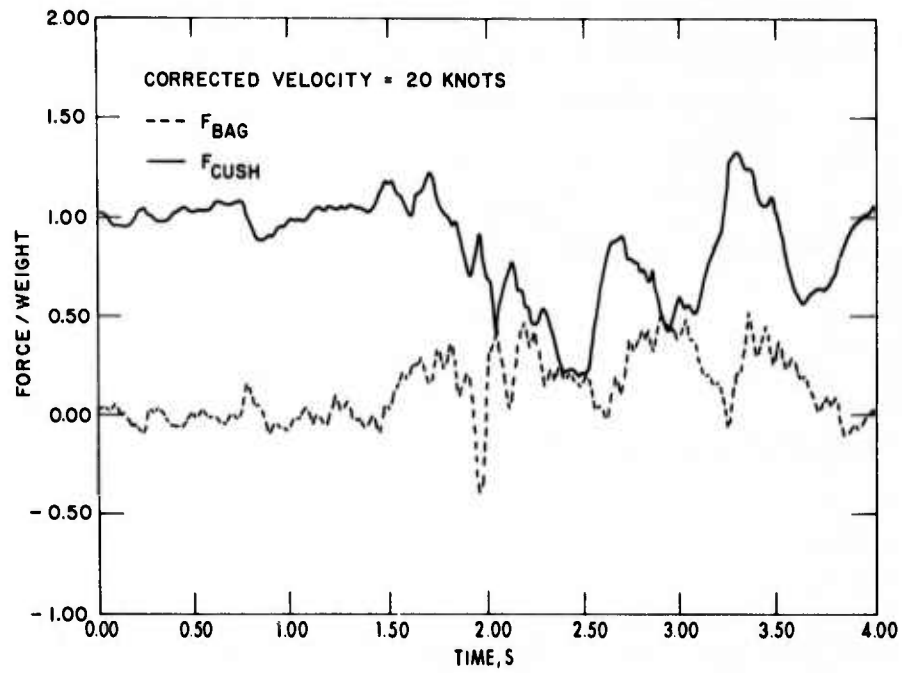


Figure 3-A
 Bag/Cushion Heave Forces and Pitch Moments
 4-Foot Obstacles (20 Knots)

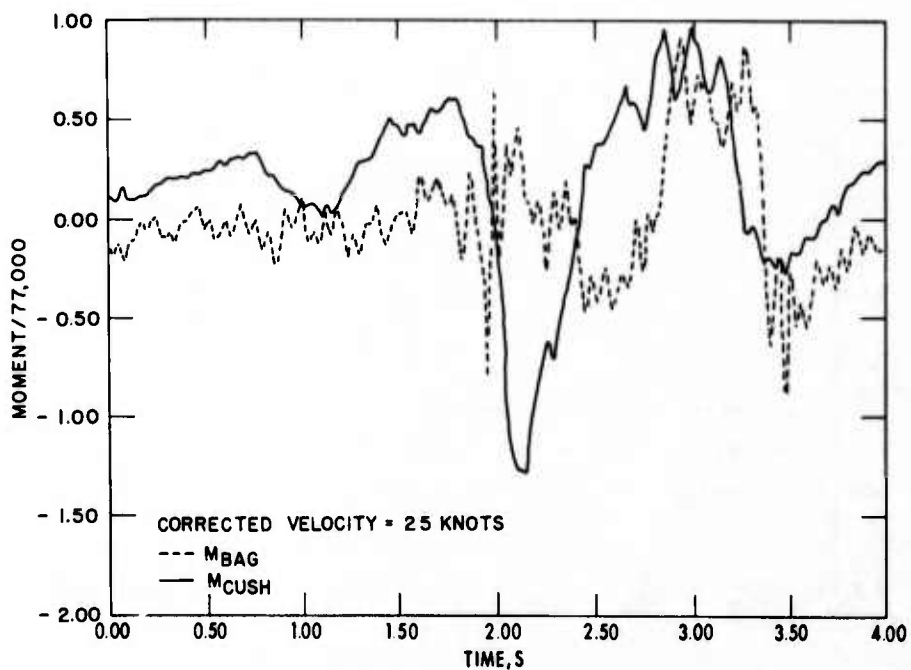
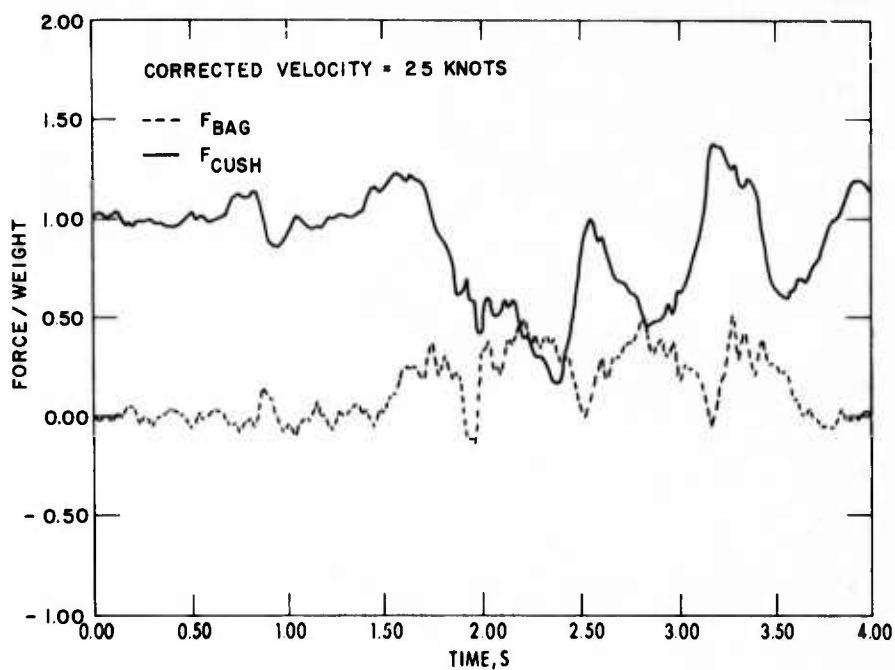


Figure 4-A
 Bag/Cushion Heave Forces and Pitch Moments
 4-Foot Obstacles (25 Knots)

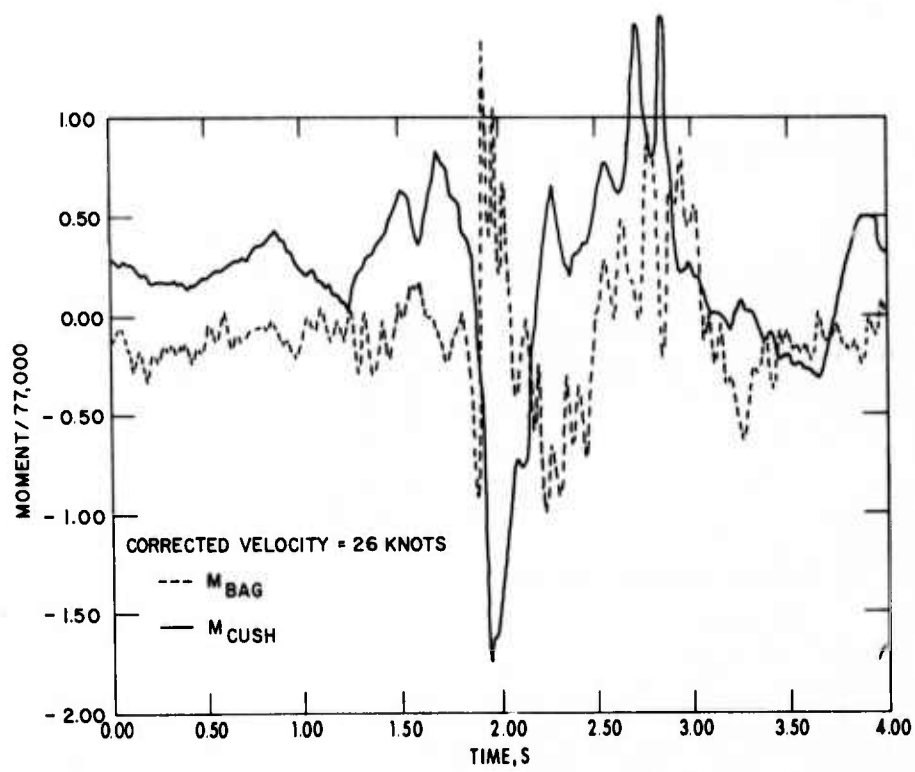
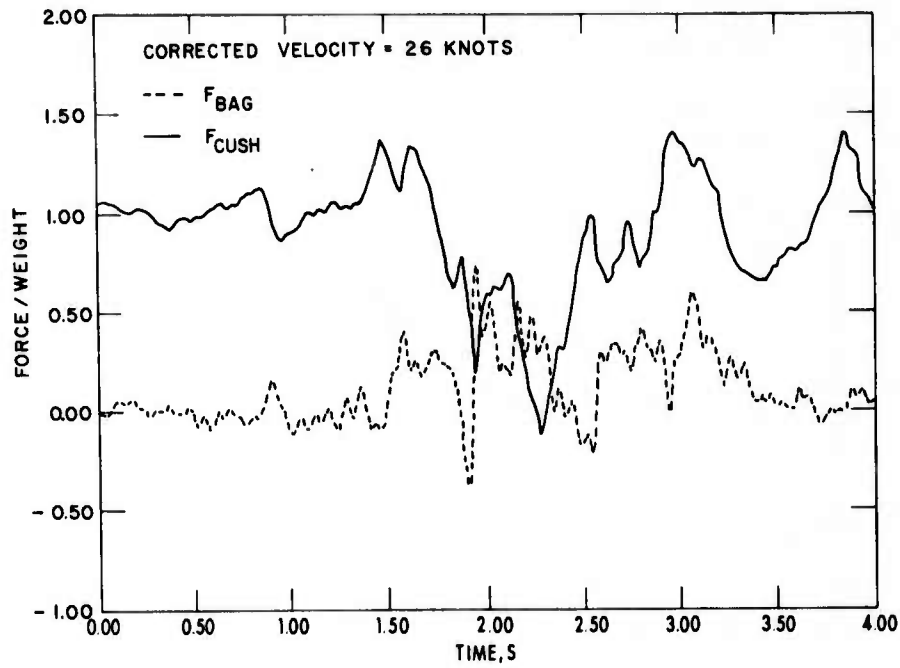


Figure 5-A
Bag/Cushion Heave Forces and Pitch Moments
4-Foot Obstacles (26 Knots)

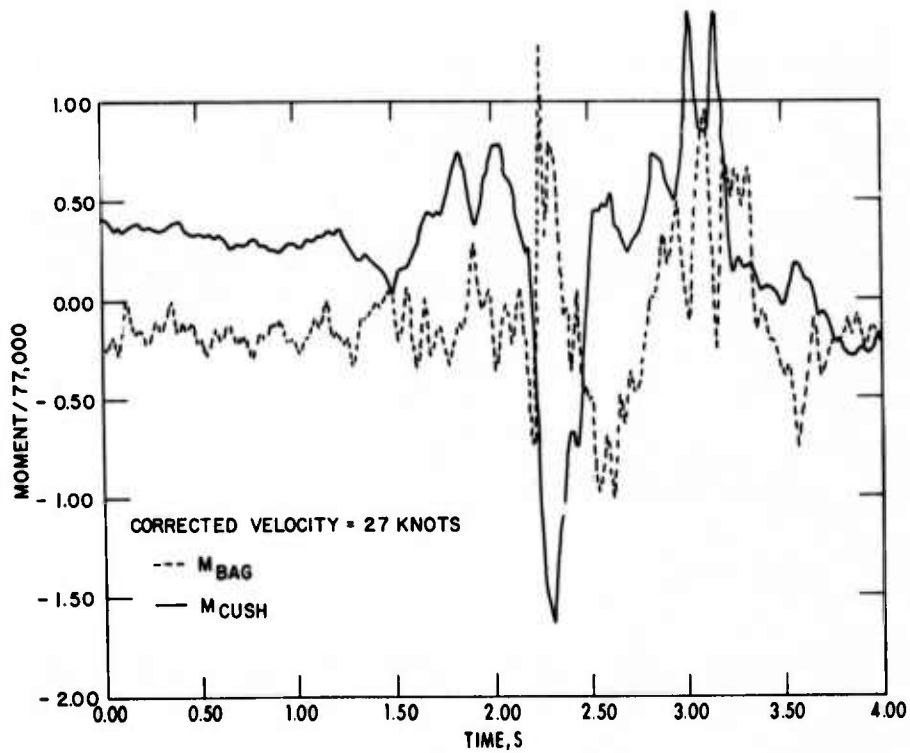
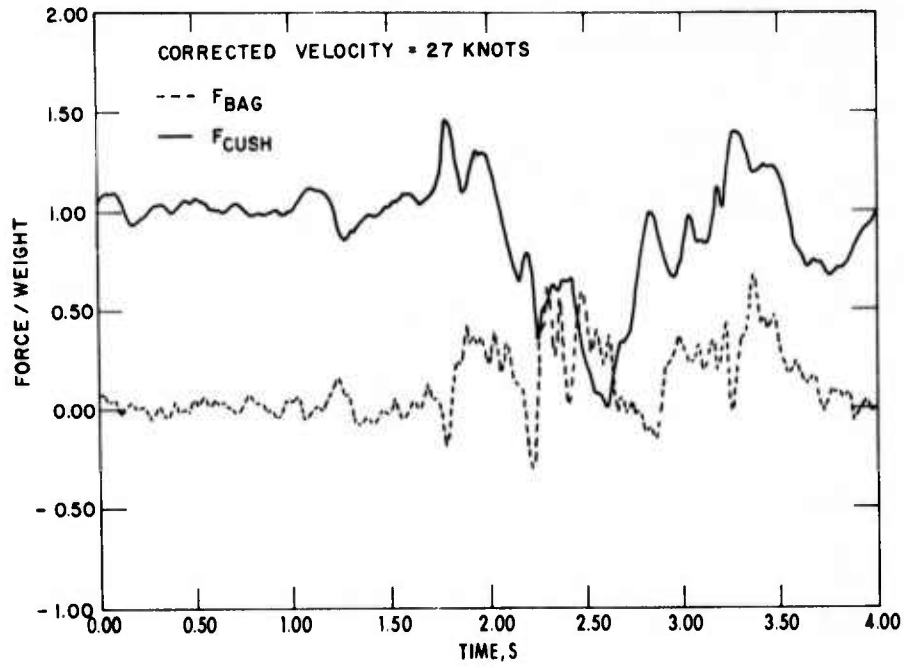


Figure 6-A
 Bag/Cushion Heave Forces and Pitch Moments
 4-Foot Obstacles (27 Knots)

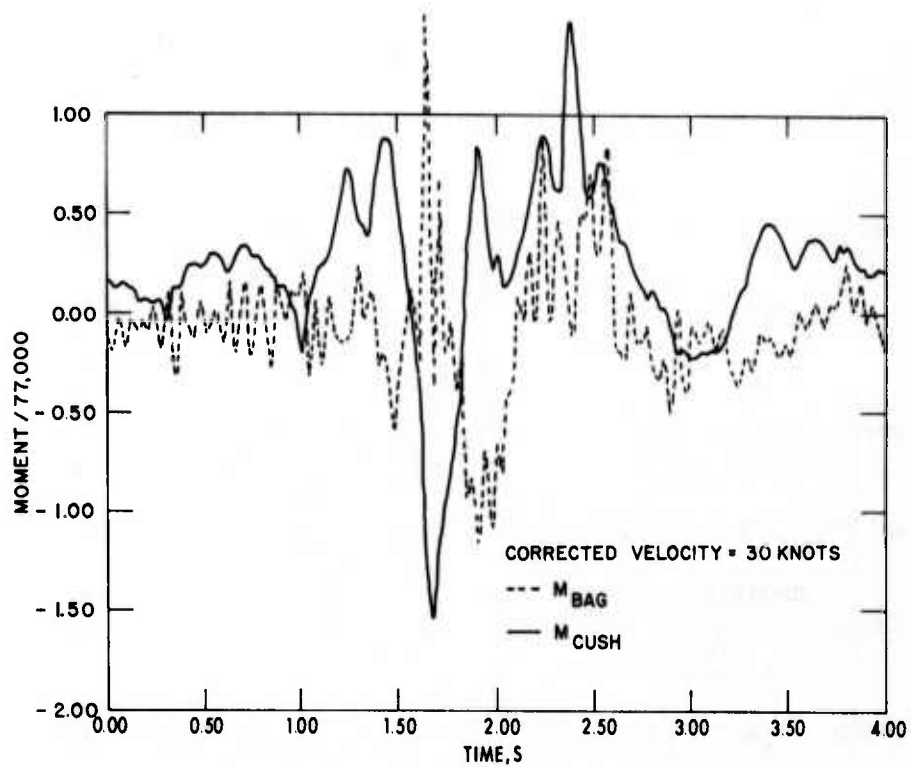
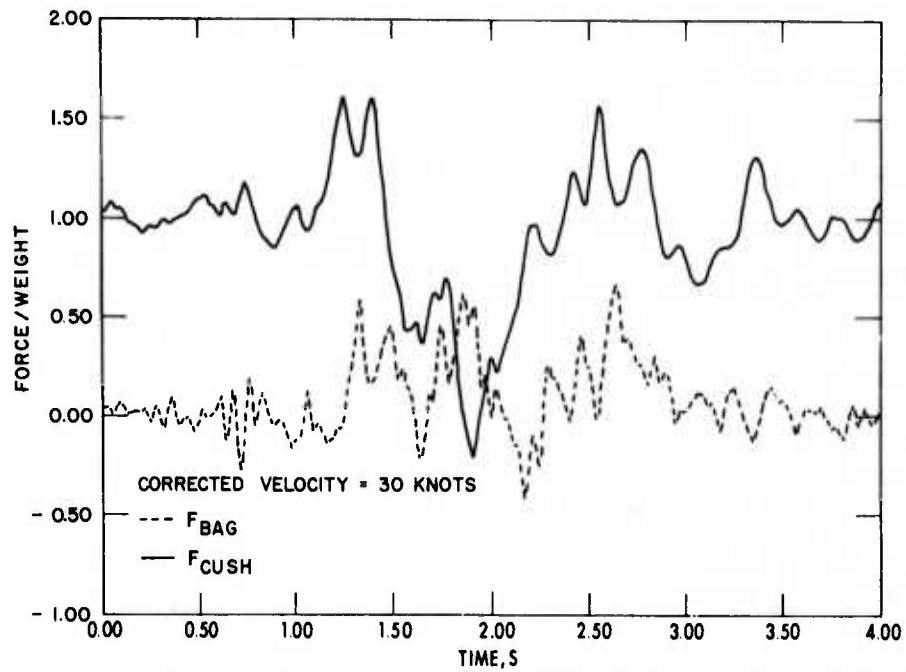


Figure 7-A
 Bag/Cushion Heave Forces and Pitch Moments
 4-Foot Obstacles (30 Knots)

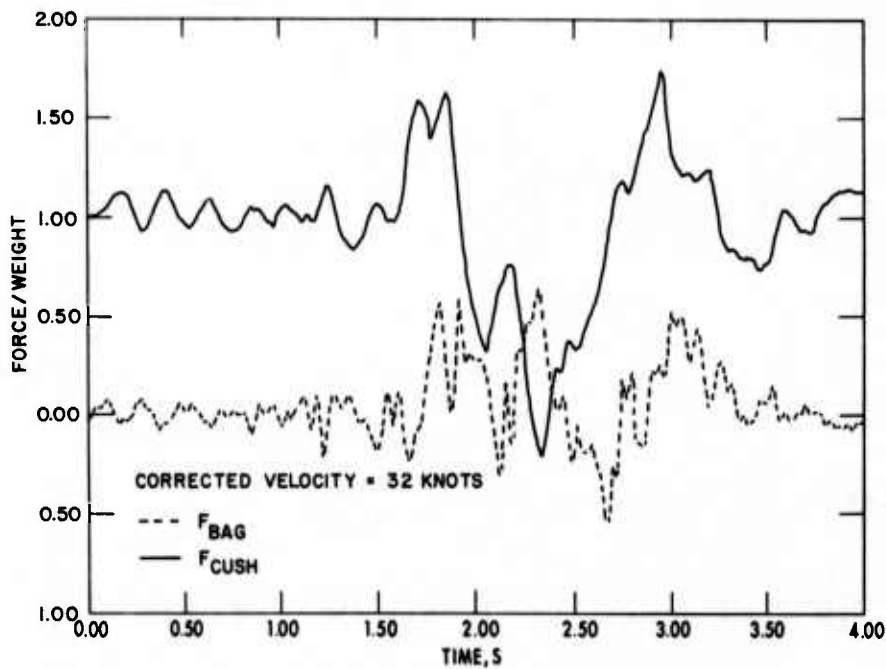
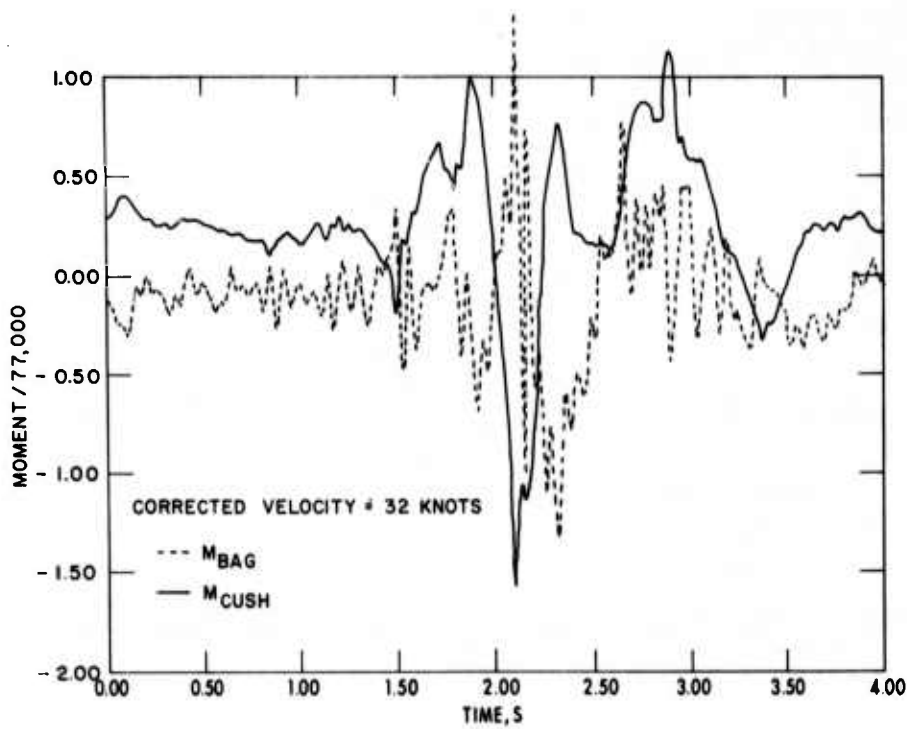


Figure 8-A
 Bag/Cushion Heave Forces and Pitch Moments
 4-Foot Obstacles (32 Knots)

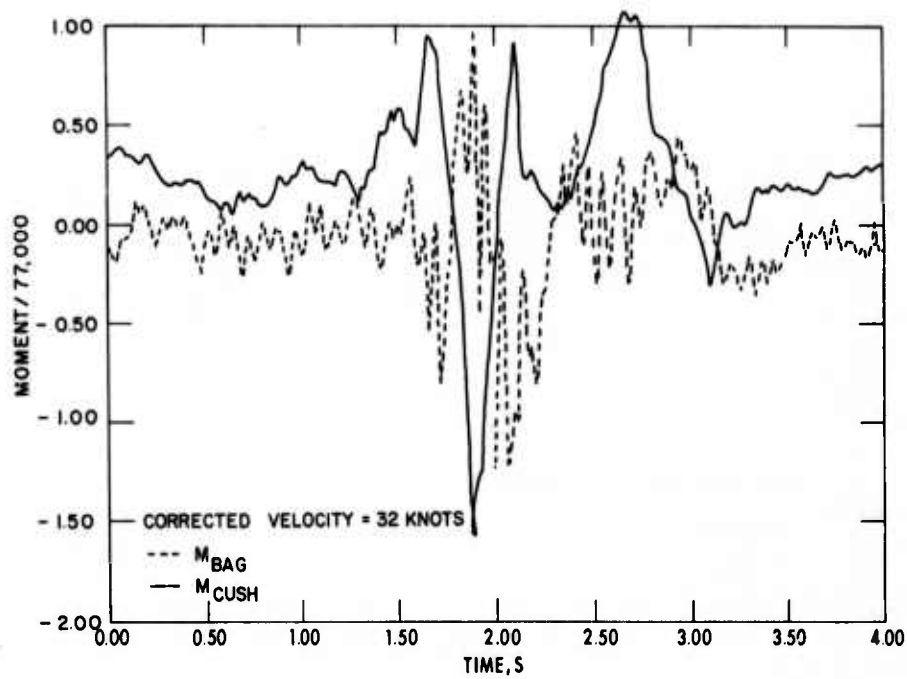
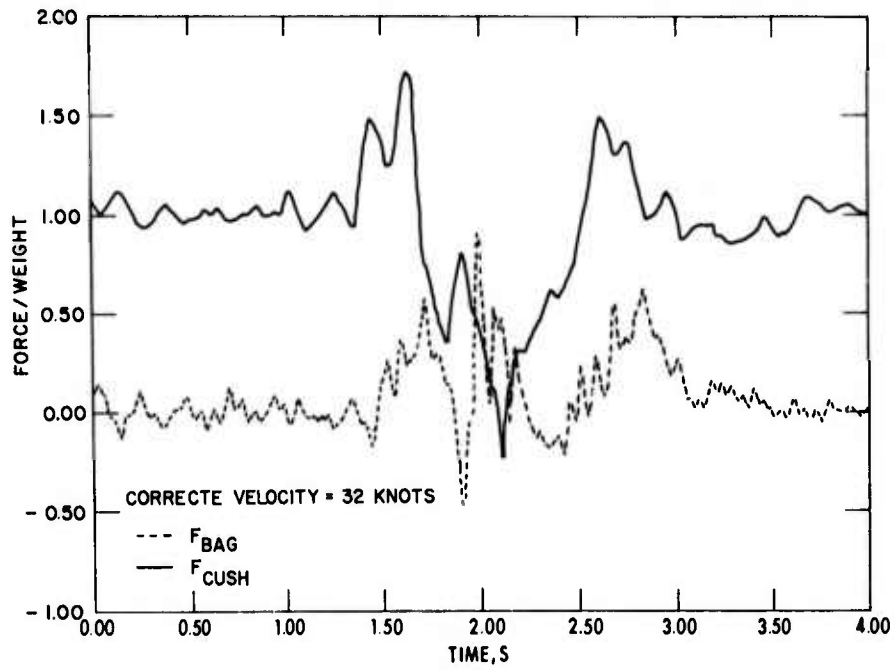


Figure 9-A
 Bag/Cushion Heave Forces and Pitch Moments
 4-Foot Obstacles (32 Knots)

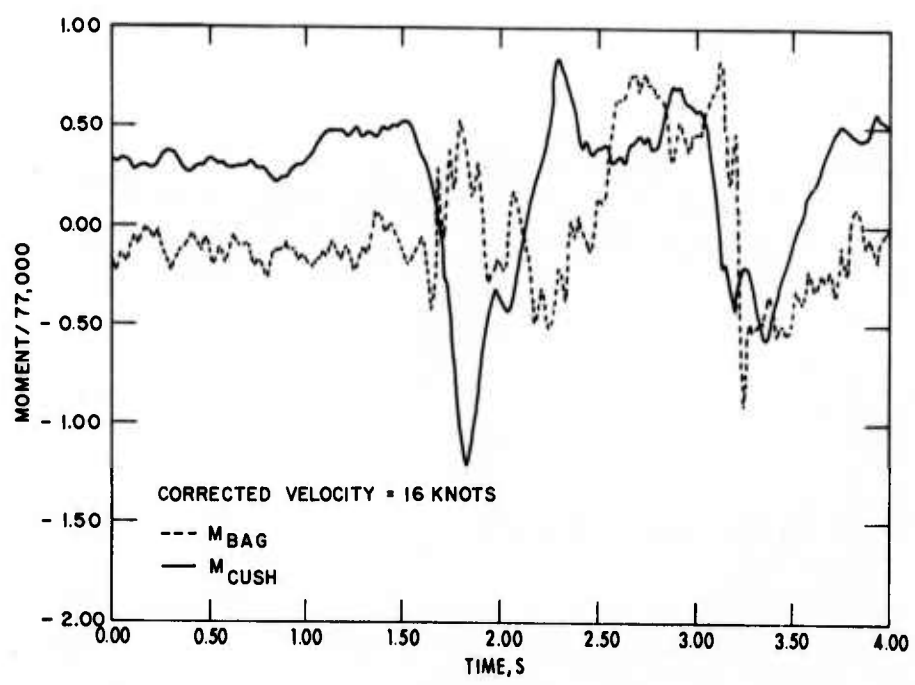
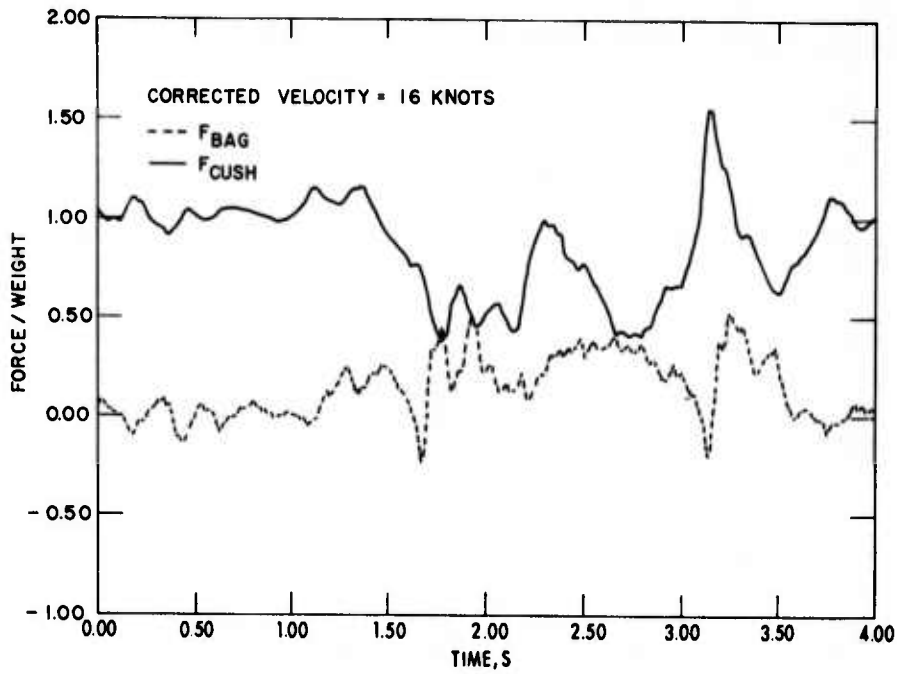


Figure 10-A
 Bag/Cushion Heave Forces and Pitch Moments
 4-Foot Obstacles (16 Knots)

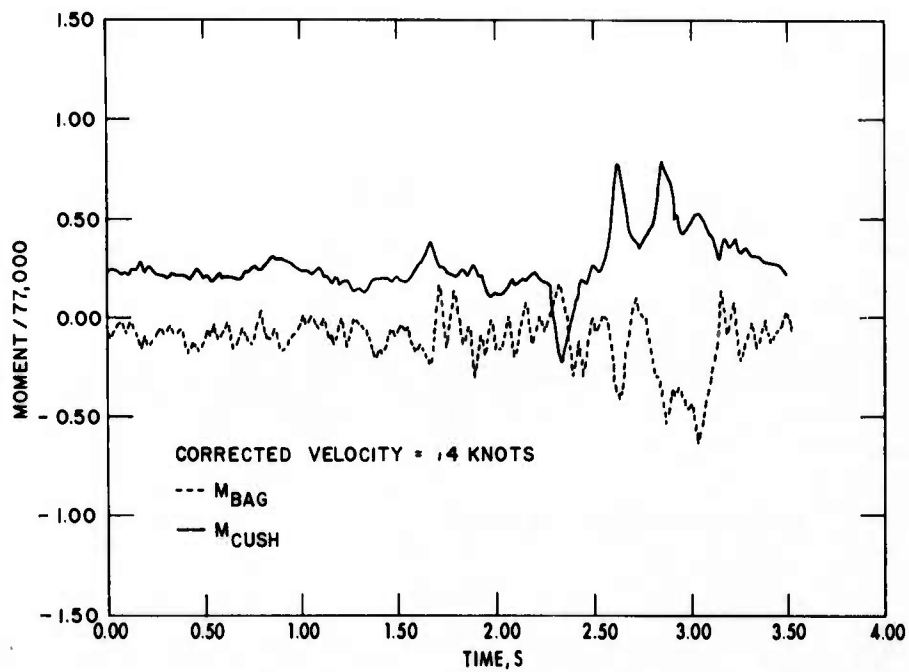
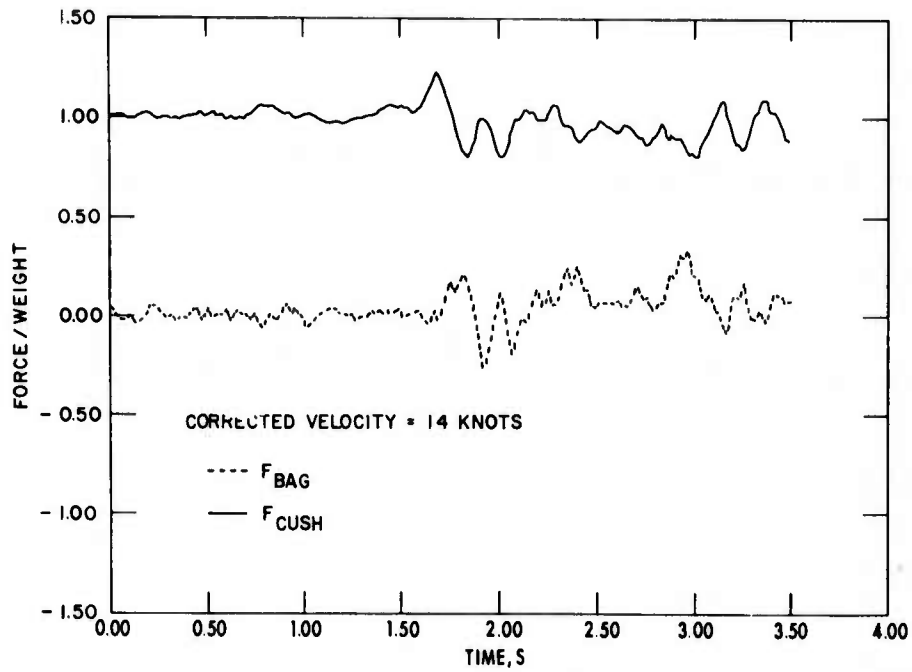


Figure 11-A
 Bag/Cushion Heave Forces and Pitch Moments
 2-Foot Obstacles (14 Knots)

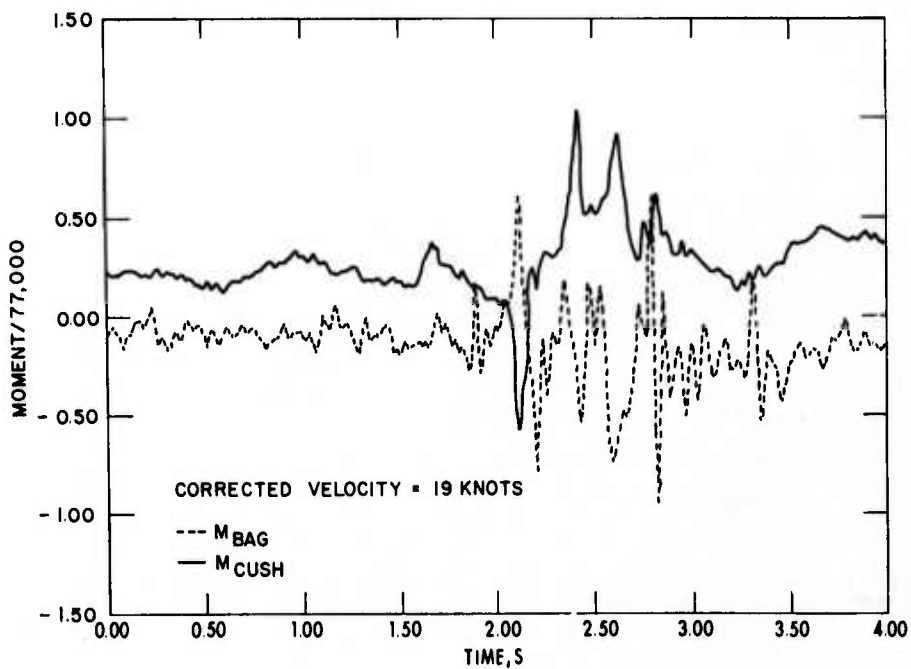
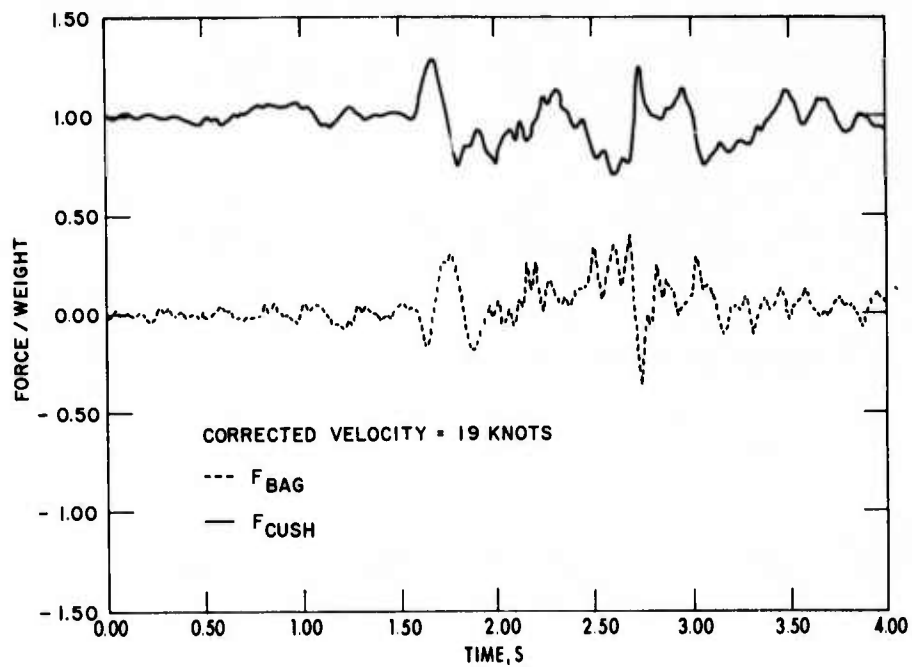


Figure 12-A
 Bag/Cushion Heave Forces and Pitch Moments
 2-Foot Obstacles (19 Knots)

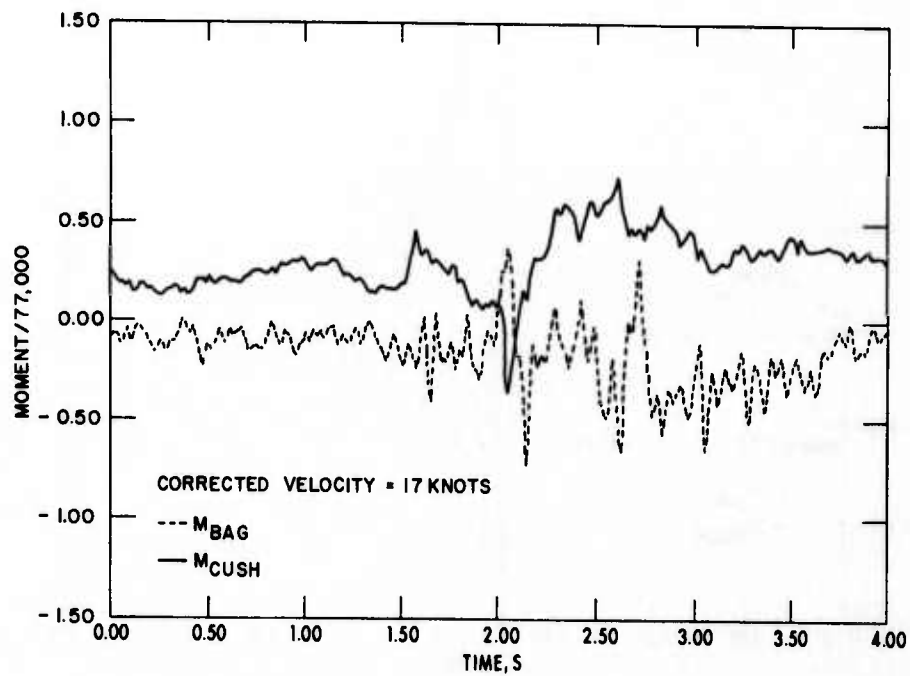
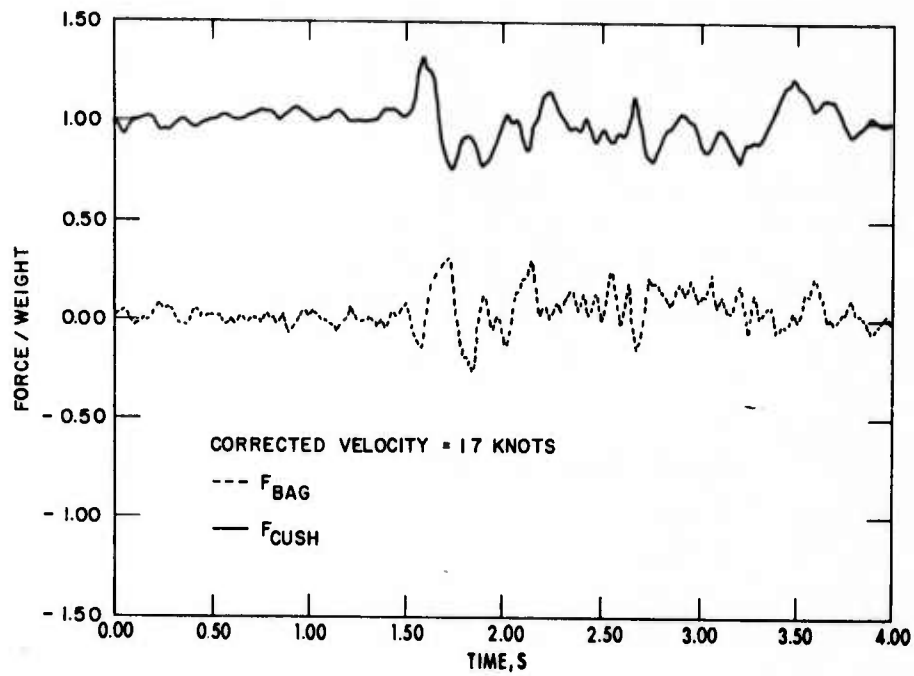


Figure 13-A
 Bag/Cushion Heave Forces and Pitch Moments
 2-Foot Obstacles (17 Knots)

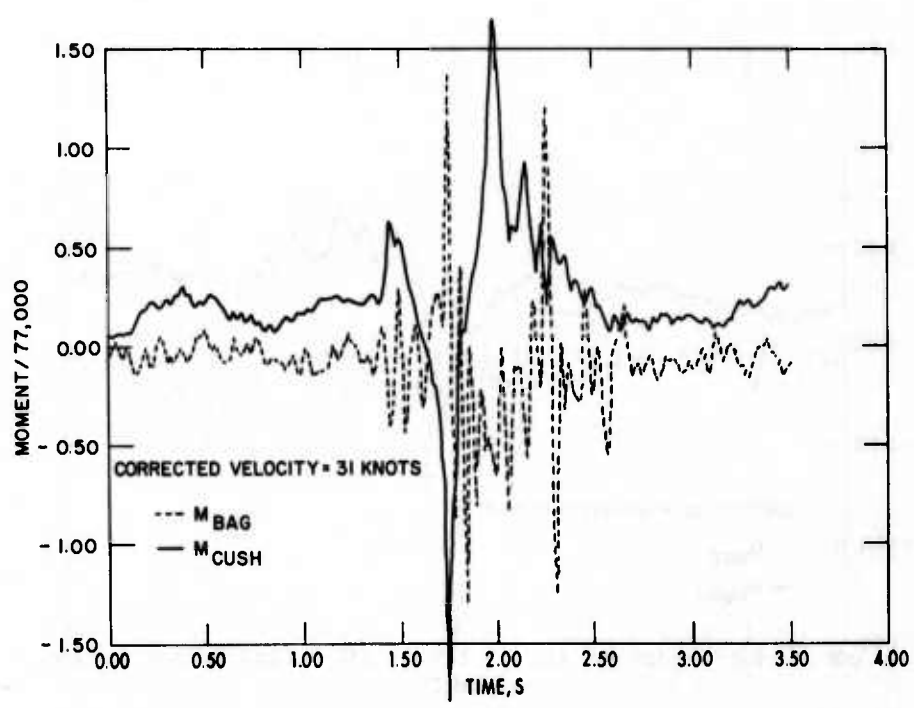
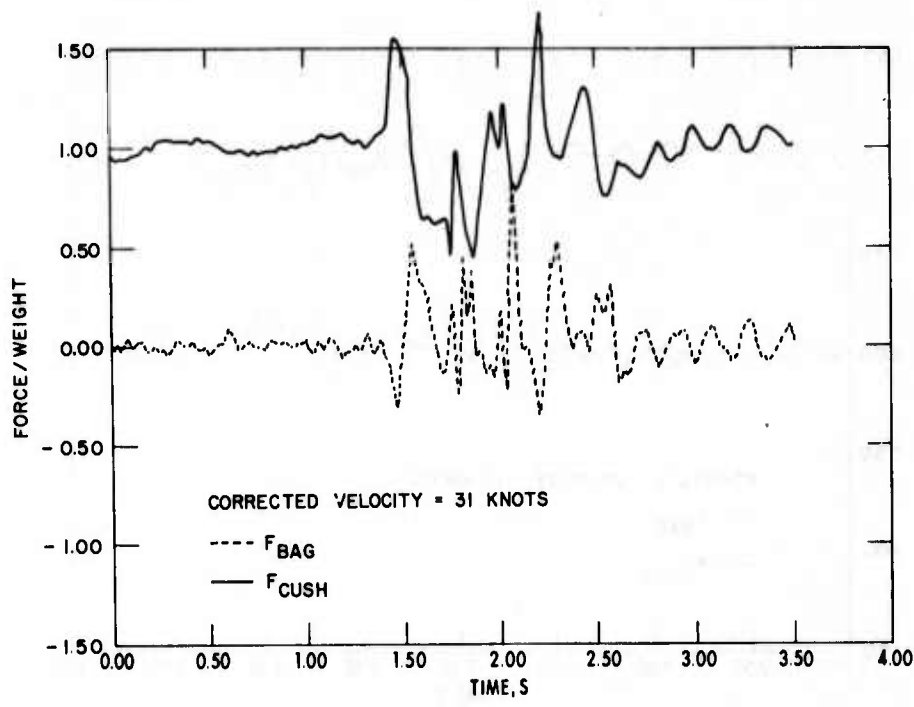


Figure 14-A
 Bag/Cushion Heave Forces and Pitch Moments
 2-Foot Obstacles (31 Knots)

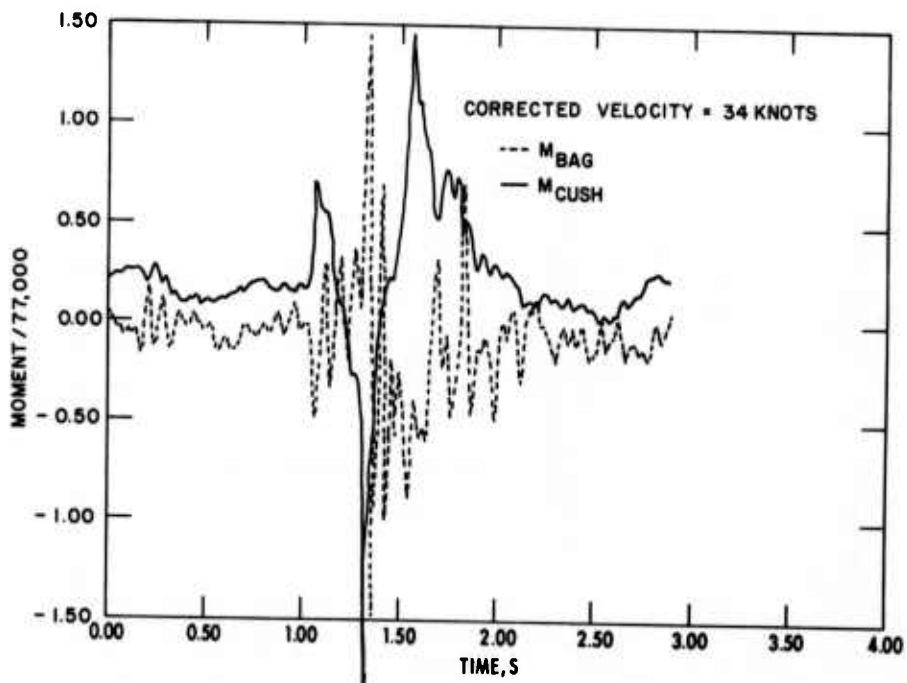
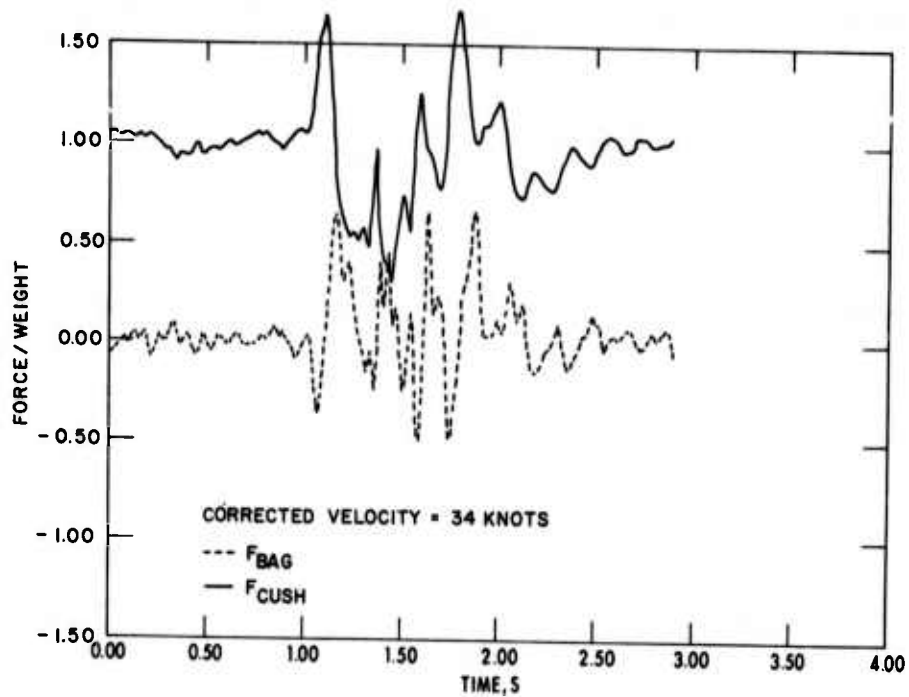


Figure 15-A
 Bag/Cushion Heave Forces and Pitch Moments
 2-Foot Obstacles (34 Knots)

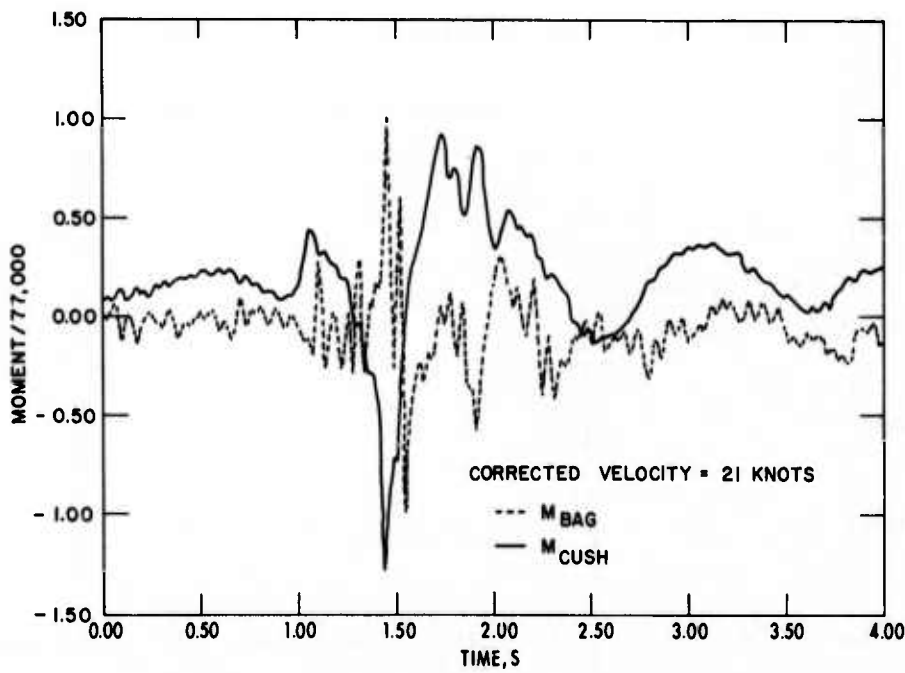
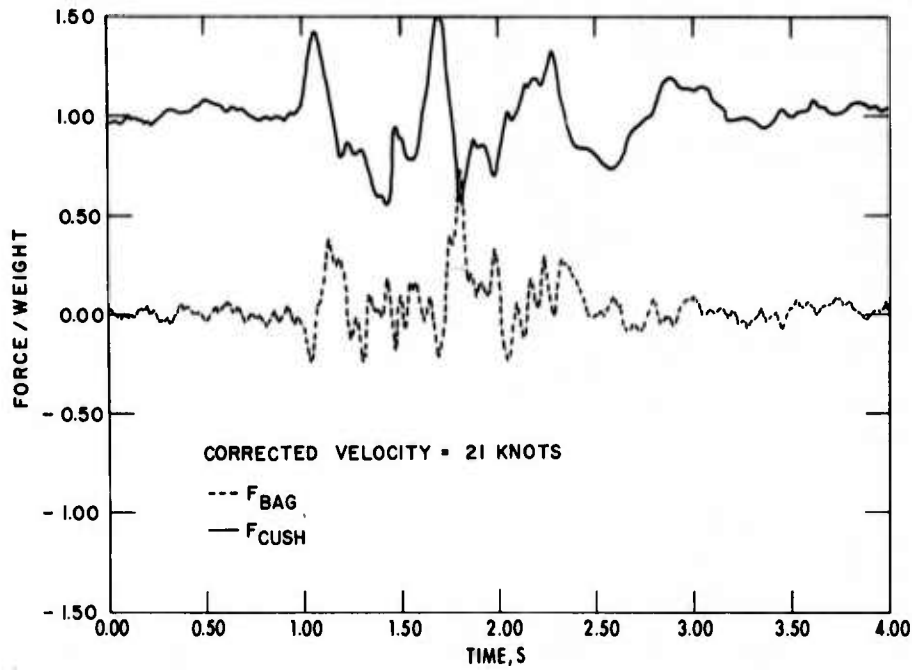


Figure 16-A
 Bag/Cushion Heave Forces and Pitch Moments
 2-Foot Obstacles (21 Knots)

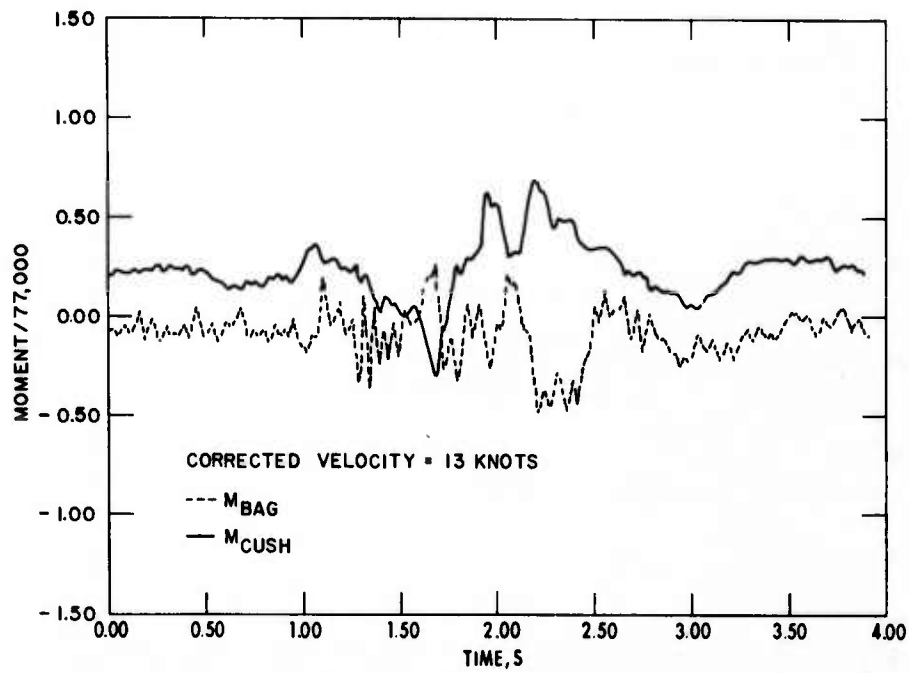
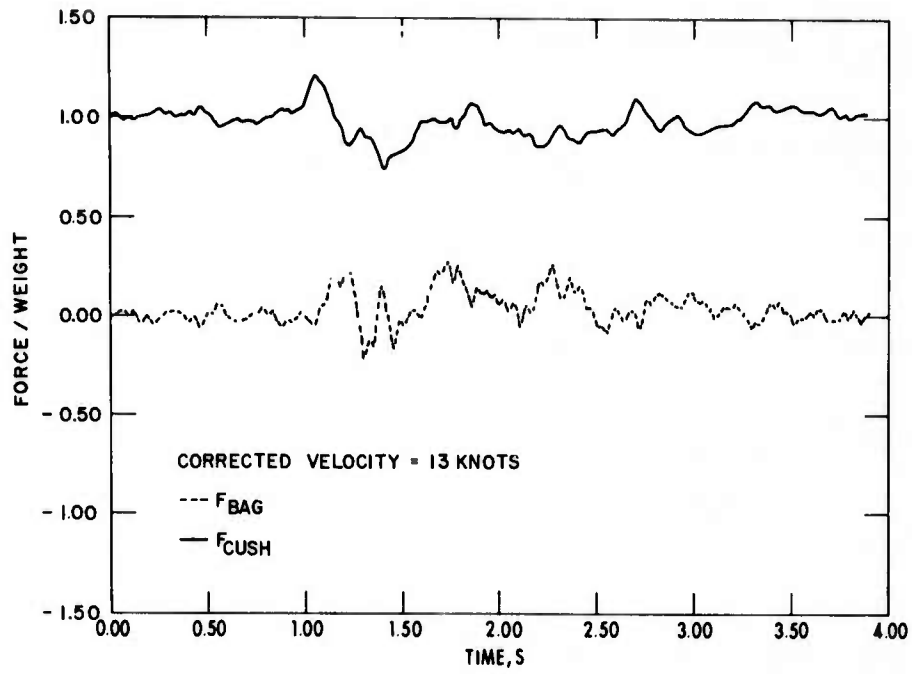


Figure 17-A
 Bag/Cushion Heave Forces and Pitch Moments
 2-Foot Obstacle (13 Knots)

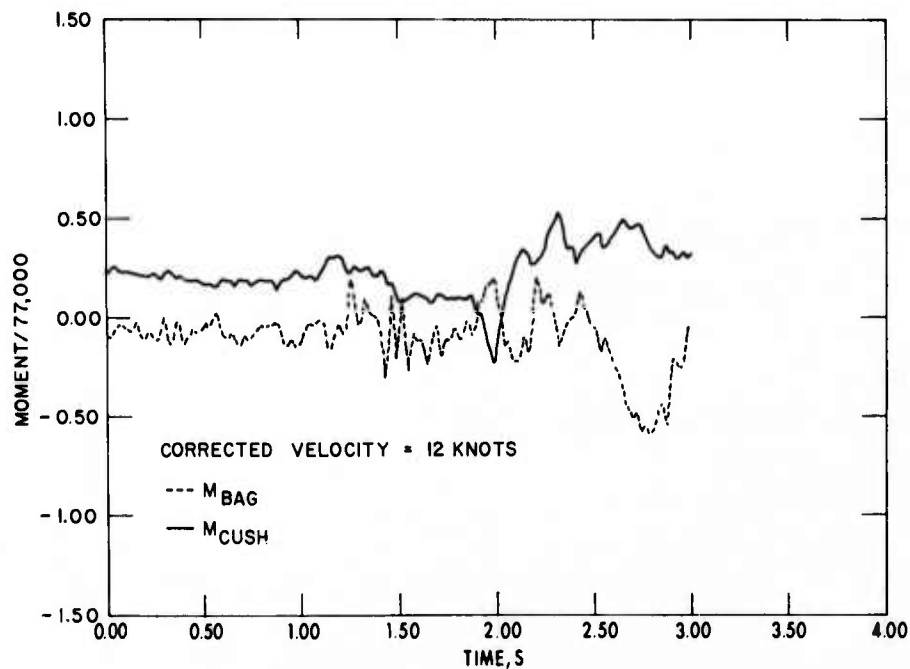
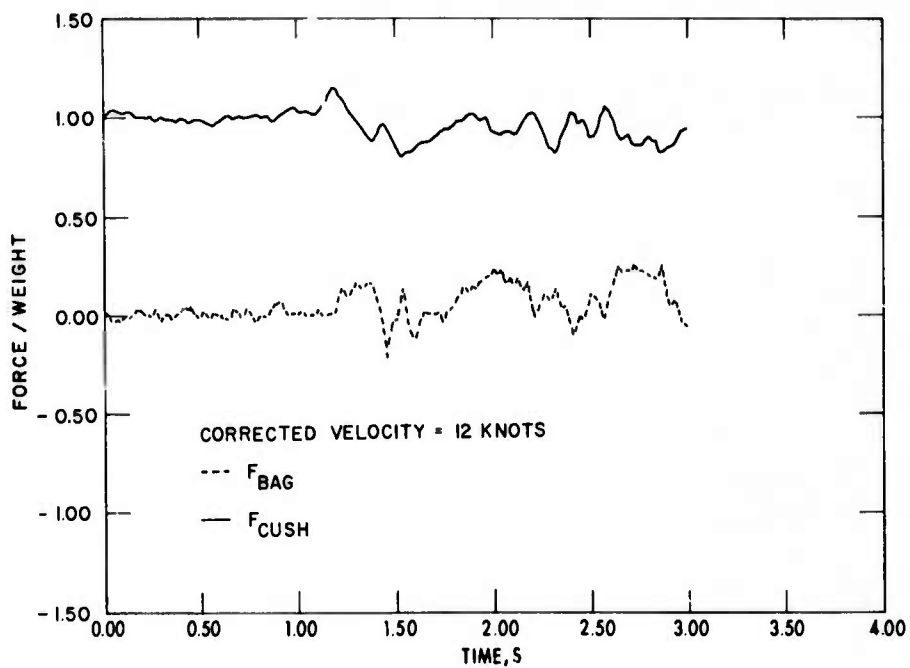


Figure 18-A
 Bag/Cushion Heave Forces and Pitch Moments
 2-Foot Obstacles (12 Knots)

INITIAL DISTRIBUTION

Copies

CENTER DISTRIBUTION

Copies		Copies	
1	OASN (Cdr. A. Smith)	1	(11) (W.M. Ellsworth)
1	ONR (Code 415)	3	(113) (J.U. Kordenbrock)
4	ARPA (Robert M. Chapman)*	1	(115) (R.J. Johnston)
1	U.S. Marine Corps (RD&S)	1	(118) (M.W. Brown)
1	U.S. Marine Corps (Dev. & Ed. Comm.)	1	(1572) (Mrs. M. Ochi)
5	NAVSEA	1	(161) (R.L. Schaeffer)
	1 (SEA 031)	3	(1735) (R.G. Allen)
	1 (SEA 03Z2)	1	(272) (Dr. E. Quandt)
	1 (SEA 03421)	10	(2721) (S.R. Shank)
	2 (SEA 2052)	1	(2803) (J.J. Kelly)
1	SESPO (PM 17)	1	(5642)
1	NAVAIR (Code 303B)	1	(5811.1)
1	NAVSEC (SEC 6110.10)	1	(9401) (Capt C.J. Boyd)
1	NELC (D. Forbes)		
1	U.S. Army, MERDC (M&BD) (J. Sargent)		
1	U.S. Army, Res. Office (Dr. V. Zadnik)		
1	U.S. Air Force, FDL (FEM) (Dr. K.H. Digges)		
1	U.S. Air Force Academy (R.W. Gallington)		
1	U.S. Coast Guard Hdqtrs (R&D)		
1	DOT, High Speed Ground Transportation (Mr. A.F. Lampros)		

* Addressee

INITIAL DISTRIBUTION (Cont)

Copies

- 1 DOT, Office of Research and Technology
- 1 SAMSO (LCol. N.F. Finnegan)
- 1 NASA Hdqtrs
- 1 U.S. Naval Academy (J.F. Sladky, Jr.)
- 2 DDC
- 1 Aerojet General Corp. (Mr. Shenfil)
- 1 Aerospace Corp. (Mr. R.T. Scott)
- 1 Bell Aerospace Co. (Mr. Hite)
- 1 Boeing Co. (Mr. Miller)
- 1 Booz-Allen Applied Research, Inc. (Mr. Willard)
- 1 Daedalean Associates (Mr. A. Thiruvengadam)
- 1 Goodyear Aerospace Corp. (Mr. Cross)
- 1 Grumman Aerospace Corp. (Mr. Munz)
- 1 Hamilton Standard (Mr. Deabler)
- 1 Oceanics, Inc. (Mr. Kaplan)
- 1 Science Applications, Inc. (Dr. C. Whittenberry)

Copies

- 1 Cornell Univ. (Dr. S.F. Shen)
- 1 Johns Hopkins Univ. Applied Physics Lab. (Mr. Paddison)
- 1 Univ. of Washington (G. Gray)
- 1 Robert S. Ross 9361 Brandywine Road Northfield, Oh 44067
- 1 Dr. M.G. Bekker 224 East Islay Santa Barbara, Ca 93101
- 1 USA, Cold Regions R&D Lab (Dr. K.L. Sterrett)
- 1 Arctic Inst. of North America (Mr. R. Faylor)